Further Reflections on Computer Modeling for Detectability Assessment of the Transition Zone in the Basement Complex Terrain of Southwest Nigeria.

Lawrence O. Ademilua, Ph.D.[1*] and Martins O. Olorunfemi, Ph.D.[2]

[1]Department of Geology, University of Ado-Ekiti, Nigeria.
[2]Department of Geology, Obafemi Awolowo University, Ile-Ife, Nigeria.

E-mail: adeoladimeji@yahoo.com[*]
mlorunfe@yahoo.co.uk

ABSTRACT

The main objective of this research is to constrain the earlier results from the works of Ademilua (2007) and Ademilua and Olorunfemi (2010) on modeling and interpretation of the parametric VES with borehole lithological logs as a further step to confirm the validity or otherwise of the earlier works as a means of offering good resolution to the detectability question as regards the basement transition zone. This is because the zone, which has remarkable significance in hydrogeological as well as engineering construction concerns, has the tendency to be suppressed on the Vertical Electrical Sounding (VES) curve due to its intermediate resistivity and often thin thickness.

The research approach has been to obtain fifteen VES datasets from locations that have been drilled and with accompanying borehole driller's logs. The resulting parameters from the analyses of the VES and borehole records were used as field tests for the observations and results from the earlier works. In carrying out the analyses, the field VES data were plotted into field sounding curves using the developed forward modeling software BABRES 1.0. The curves, as usual, were studied for signatures of the transition zone. The drag lengths were measured and recorded for curves displaying evidence of the transition zone, From these it was observed that the transition zone becomes detectable with a thickness ratio (between it and the overlying layers) not less than 0.73 for the HA- and 1.11 for the KHA- type curves. Also, it was discovered that the resistivity ratios (between it and immediate overlying layer) permitting detectability range between 1.67 to 3.67 for the HA-type, and 1.67 to 4.33 for the KHA-type curves. Below these ranges the zone becomes undetectable.

These findings are not only supportive, but confirmatory of the results from the said earlier works of Ademilua (2007) and Ademilua and Olorunfemi (2010). It can thus be concluded that the basement transition zones are only detectable within certain limits of thickness and resistivity ratios.

(Keywords: basement profile, resistivity ratio, computer software, horizons, detectable, thickness ratio, borehole, VES)

INTRODUCTION

The crystalline basement rocks are generally massive and impermeable, the boundary between the weathered layer and the fresh basement bedrock is rarely sharp. Most often a transition zone, referred to by Mcfarlane (1989) as the saprock exists between the weathered layer and the fresh basement (Figure 1).

In a typical basement complex environment, the transition zone has been identified as a very important lithologic unit which contributes significantly to the prolificity and yields of groundwater boreholes. Because of its enhanced permeability due to secondary porosity, the transition zone complements the weathered layer in terms of groundwater storage and yields. This zone of fracturing below the saprolite (transition zone) as earlier discussed forms an aquifer in addition to the overlying weathered layer (saprolite). This aquifer combination is called weathered/fractured (unconfined) aquifer (Olorunfemi and Fasuyi 1993; Ademilua, 1997; Ademilua and Olorunfemi 2002 and Idornigie, 2005). Statistical analysis of borehole logs and yields in the basement complex (Table 1) indicated that higher average yields were achieved by holes which crossed the brecciated

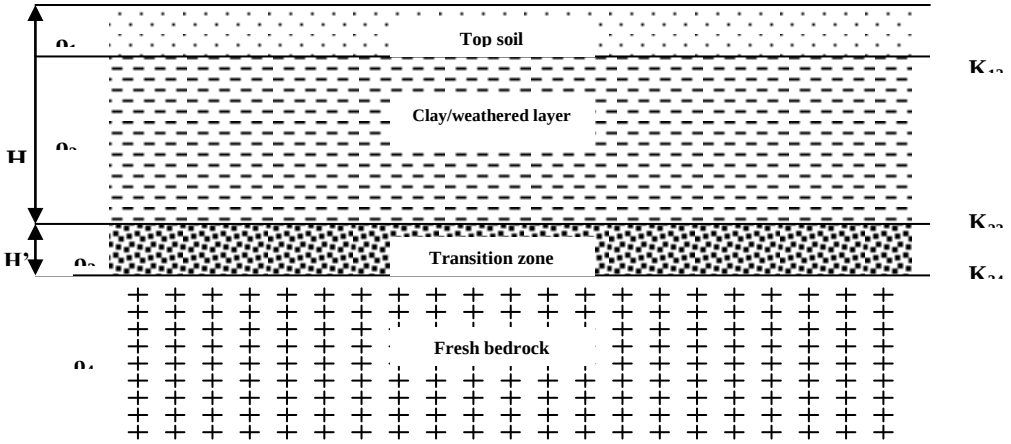

Figure1: Model of a Typical 4-layer Earth in the Basement Complex Area.

Table 1: Aquifer Types and Borehole Yields in the Basement Complex Areas of Ekiti and Ondo States S. W. Nigeria (after Ademilua, 1997).

S/No	Aquifer Types	Borehole Yields Range (L/s).	Mean Yield
1.	Weathered layer Aquifer	0.51	0.51
2.	Weathered/fractured (unconfined) Aquifer	1.39 – 1.86	1.63
3.	Weathered/fractured (confined) Aquifer	0.33 – 2.39	1.43
4.	Weathered/Fractured (unconfined)/Fractured (confined) Aquifer	0.47 – 10.00	3.16
5.	Fractured (Confined) Aquifer	0.47 – 3.53	1.74

zones as compared with holes which stopped in the regolith before reaching the zone (MacFarlane, 1989; Olorunfemi and Fasuyi, 1993; Ademilua 1997).

With appreciable thickness of the transition zone and enhanced permeability, boreholes which penetrate the zone give good yield. It follows therefore that significant groundwater yield is only gotten in basement complex area when the borehole straddle the transition zone. This makes the identification of the zone very important in most hydrogeological campaigns in the basement complex environments.

However, in the engineering and construction works, it is a zone of interest because of its negative impacts on foundation structures as a potential seepage zone. The basement transition zone impacts negatively on most engineering structures since it serves as possible seepage zone which poses great threat to the foundation of such structures. The Nassarawa earth dam embankment which was founded on a basement rock with high density planar/angular fractures and joint systems failed because of subsurface seepage which seriously undermined the foundation of the existing spillway structure (Ojo et al., 1990; Olorunfemi et al., 2003; Ajayi et al., 2006). Such zone could also serve as seepage path for leachates generated in landfill sites located in basement complex area (Western, 1997).

However, this zone may often not be easily detected on the Vertical Electrical Sounding (VES) curve due to suppression, there is therefore the need to undertake an in-depth study on the detectability of the zone on the VES curve as a means of enhancing its delineation and correct interpretation. In areas underlain directly by crystalline basement rocks, the inversion of vertical electrical sounding data is non – unique in terms of the ability to reliably estimate the depth to bedrock and possibly detect the zone of fracturing below the saprolite (Hazel et. al., 1992; Barker et al., 1992; Caruthers and Smith, 1992).

A generalized geoelectric model involving a basement transition zone is composed of four layers; a topsoil, weathered layer, partly weathered/fractured (transition zone) and the fresh basement. The resistivity (ρ) combination is of the form $\rho_1 > \rho_2 < \rho_3 < \rho_4$ with an HA-type curve. Where the topsoil is composed of more than one layer, a KHA- or QHA- type curve could be obtained (Ademilua, 1997). On the VES curve, the transition zone manifests as a gentle drag along the rising (basement) segment of the HA-type (Figure 2) or KHA-or QHA-type curves .The existence of the zone introduces a drag along the rising (basement) segment of the curve, thus dividing the segment into two parts. The drag constitutes the first part of the rising segment whose inclination is $<<45^0$, while the second part which rises at an angle of 45^0 constitutes the fresh basement. However, the HA-type is the most common in the Basement Complex environment (Olayinka and Oladipo, 1994).

Therefore, the uniqueness and importance of the transition zone amongst other subsurface lithological units in the basement terrain, in terms of (i) groundwater exploration and general hydrogeology, and (ii) engineering foundation design construction/environmental studies cannot be overemphasized.

RESEARCH METHODS

(i) Background/Previous Approach

The authors had earlier used an interactive computer software (BABRES 1.0) developed by them (Ademilua,2007;Ademilua and Olorunfemi 2007) for Schlumberger resistivity forward modelling of various geologic models involving the transition zone in Ademilua and Olorunfemi (2010) . To achieve this, they carried out theoretical VES computer modelling of basement profile containing the transition zone (or saprock) with varying thicknesses and resistivities as a means of assessing the detectability of the hydrogeologically important zone with often thin layer.

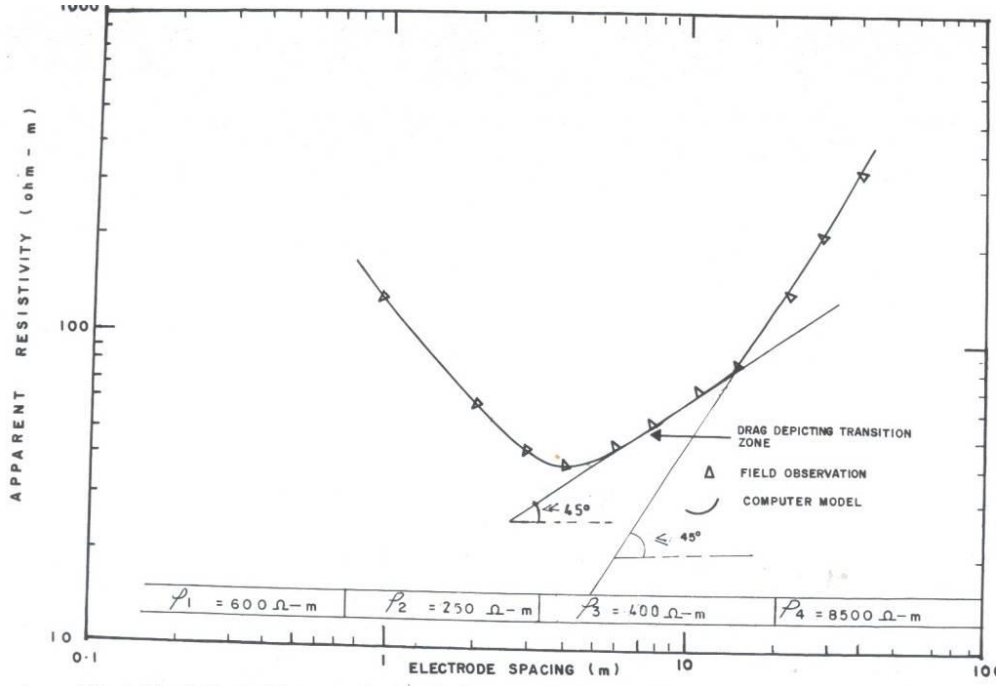

Figure 2: Geoelectric Signatures of a Basement Complex Profile Containing the Transition Zone (culled from Ademilua, 2007; Ademilua and Olorunfemi, 2010).

The forward modeling software (BABRES 1.0) was used to facilitate the generation of series of four-layer HA- and five-layer KHA- type model curves depicting the situation. In doing this, two approaches were adopted; In the first approach, for fixed values of the resistivities and thicknesses of the other three layers (for HA-type curves), the thickness of the transition zone was varied in step of 2m between 2m and 50m for a given transition zone resistivity. This is in agreement with Acworth, (1987); Buckley and Zeil, 1984; White, et al., 1988; Olayinka and Oladipo (1994) as they all posited that in crystalline basement areas, the thickness of the weathered zone is commonly less than 30m while the thickness of the topsoil layer hardly exceeds about 2m. Therefore, the thickness of the topsoil was fixed at 1m, that of the weathered layer was put at 10m, while the transition zone's thickness was put at 2 m for the starting model. The layer resistivity values were fixed at 500 ohm-m, 150ohm-m, 300ohm-m and 10,00ohm-m respectively (see Appendices 1- 4 for representative samples of typical models generated for the HA- type curve).

This procedure was also followed in the case of the case of the KHA-type curves except that the thickness of the transition zone was varied in step of 5m between 5m and 80m for a given transition zone resistivity, while the layer resistivity values were fixed at 200 ohm-m,750 ohm-m,150 ohm-m,250 ohm-m and 10000ohm-m respectively for the horizons. For each of the resulting parameter set from the variations, a model curve was generated (see Appendices 5–8 for representative samples of typical models generated for the KHA- type curve). The curves so generated were thereafter carefully examined for the signatures of the transition zone. Where this is detectable, the drag lengths (in cm) which is the linear extent of the transition zone as detected within the rising segment of the curve were measured , so also was the drag angle β^{o} which a tangential line drawn at the drag surface makes with the horizontal axis measured and recorded.

In the second approach and for the HA-type curves, the resistivities of the other three layers were fixed while that of the transition zone was varied. The resistivity was varied from 250 ohm-m to 850 ohm-m for the transition zone. For the starting model, the resistivities are 500 ohm-m for topsoil, 150 ohm-m for weathered layer, 250 ohm-m for the transition zone while the fresh basement has a resistivity of 10000 ohm-m. The thicknesses of the starting models are 1 m for topsoil, 10 m for weathered layer while the transition zone has a thickness of 2m (see Appendices 9- 11 for representative samples of typical models generated for the HA-type curve). Again, this procedure was repeated for the KHA-type curves except that the starting model has resistivity values of 200 ohm-m for topsoil layer, 750 ohm-m for the lateritic layer, 150 ohm-m for the weathered layer, 250 ohm-m for the transition zone and 10000 ohm-m for the fresh basement.

The thicknesses of the horizons are respectively fixed at 1m, 2.5m, and 10m for the three top layers, and 10m for the transition zone. Each of the resulting parameter sets was used to generate model curves (see Appendices 12-14 for representative samples of typical models generated for the KHA- type curve), As in the first case, the drag length was measured in curves where the zone is detectable, so also is the drag angle β^{0}. For each of the model curves allowing for detectability, the resistivity ratio of the transition zone to that of the overlying weathered layer (ρ_3/ρ_2) for the HA-, and ρ_4/ρ_3 for the KHA—type curves were calculated and recorded.

Summarily, the authors were able to use this modeling to conclude that the transition zone can only be identified on the VES curve when the ratio of the thickness of the zone to that of the overlying layers is not less than 0.73 for the HA- and 1.11 for the KHA-type curves. Also the resistivity ratio of the zone to that of the immediately overlying weathered layer must range from 1.67 to 4.33 for the HA- and 1.67 to 5.00 for the KHA-type curves. Above these ranges, the zone becomes difficult to differentiate from the fresh basement. Furthermore he concluded that, for optimum detectability, the resistivity ratio should be between 3.0 and 3.67 for the HA-type curve and 3.8 – 4.50 for the KHA-type curve.

(ii) <u>Latest Approaches</u>

Considering the earlier stated multidimensional importance of this zone, and arising from subsequent field encounters on this and related issues that bother on the transition zone, the authors feel obliged to carry out further studies on the basement transition zone's detectability on the VES curve. The objective of this study is therefore to constrain the earlier modeling and

interpretation of the parametric VES with lithological logs from boreholes as a further step to confirm the validity or otherwise of the earlier results as a means of offering good and lasting resolution to the detectability question.

Therefore in this approach, fifteen field VES datasets obtained from localities within the study area (basement complex terrain) were acquired. These data were acquired from locations that have been drilled and with accompanying borehole driller's logs. The resulting parameters from the analyses of the VES and borehole records were used as field test for the observations and results from the earlier approaches of Ademilua and Olorunfemi (2010).

In carrying out the analyses, the field VES data were plotted into field sounding curves using the developed forward modeling software BABRES 1.0. The curves, as usual, were studied for signatures of the transition zone. The drag lengths were measured and recorded for curves displaying evidence of the transition zone. The VES curves were conventionally interpreted using the partial curve matching and computer iteration technique involving BABRES 2.0. Thereafter, the geoelectric section and lithologic sections from the drillers' logs were then drawn and correlated graphically using the 'draw' facilities of Microsoft Word software and placed below the VES curve (Figures 3–17). This was done to facilitate wholesale graphical assessment of each data location amongst other reasons.

From the VES data, the resistivity ratio (RR) and the thickness ratio I (TR1) as in the earlier approaches were obtained, while the presumably "actual" thickness ratio II (TR2) was deduced from the lithologic logs. The summary of the resulting parameters from the analyses of these data are as presented in Table 2. Using these, graphs were plotted to show relationships between: (i) drag length and thickness ratios I and II, (ii) drag length and resistivity ratio for each of the two type-curves (HA- and KHA-)

RESULTS AND DISCUSSION

Arising from the model study and analysis of the field VES and borehole data, the following question arises, answer to which would facilitate a focused discussion and understanding of the results. Are the findings from the earlier studies carried out by Ademilua and Olorunfemi (2010) as summarily discussed above corroborated by the results from the analysis of the field VES and borehole lithologic logs? From Figures 3–17 and Table 2, it would be observed that at Ado–Ekiti (5) and Akure (5) locations, both the minimum thickness and resistivity ratio limits criteria were not met, hence the zone's signatures could not be seen or detected on the respective VES curves.

However, in stations like Akure (1), Osogbo and indeed in all other locations where the HA-type curves are predominant, the zone's signatures were observable on the respective curves, these are as a result of the thickness and resistivity ratios limits being observed. Furthermore, the same situations could be seen to be obtainable in the cases of the remaining locations where the KHA- type curves predominate, and that is referring to Ibadan and Akure.

The zone is detectable because both the thickness ratio and resistivity ratio limits criteria are met. Additionally, it would be observed that the effect of marginal increase in the thickness ratio does not readily impact noticeably on the drag length. Only a substantial increase would result in observable increase.

Figures 18 and 19 (culled from Ademilua and Olorunfemi, 2010), show that the drag length increases polynomially with the thickness ratio. This could be seen to be in agreement with the results of the analysis of the field VES and borehole data (Table 2). From these, it is reasonable to infer that an increase in the thickness ratio leads to an increase in the drag length.

Another inference from this is that, above the minimum detectable thickness ratio, the zone would continue to be recognized on the VES curve for the same range of resistivity ratio. From Ademilua and Olorunfemi (2010), it was shown that the transition zone could not be detected below resistivity ratio of 1.67 for both curve types,and beyond 4.33 and 5.00 for HA and KHA type curves, respectively. The drag length steadily increases with increase in resistivity ratio up to an optimum value between 3.0 and 3.67 for HA-type curve and 3.80 and 4.50 for the KHA-type curve, and subsequently decrease with increase in the resistivity ratios (see Figures 20 and 21). At these optimum values, the drag length reaches its maximum and the zone becomes mostly pronounced and easily detectable on the VES curves.

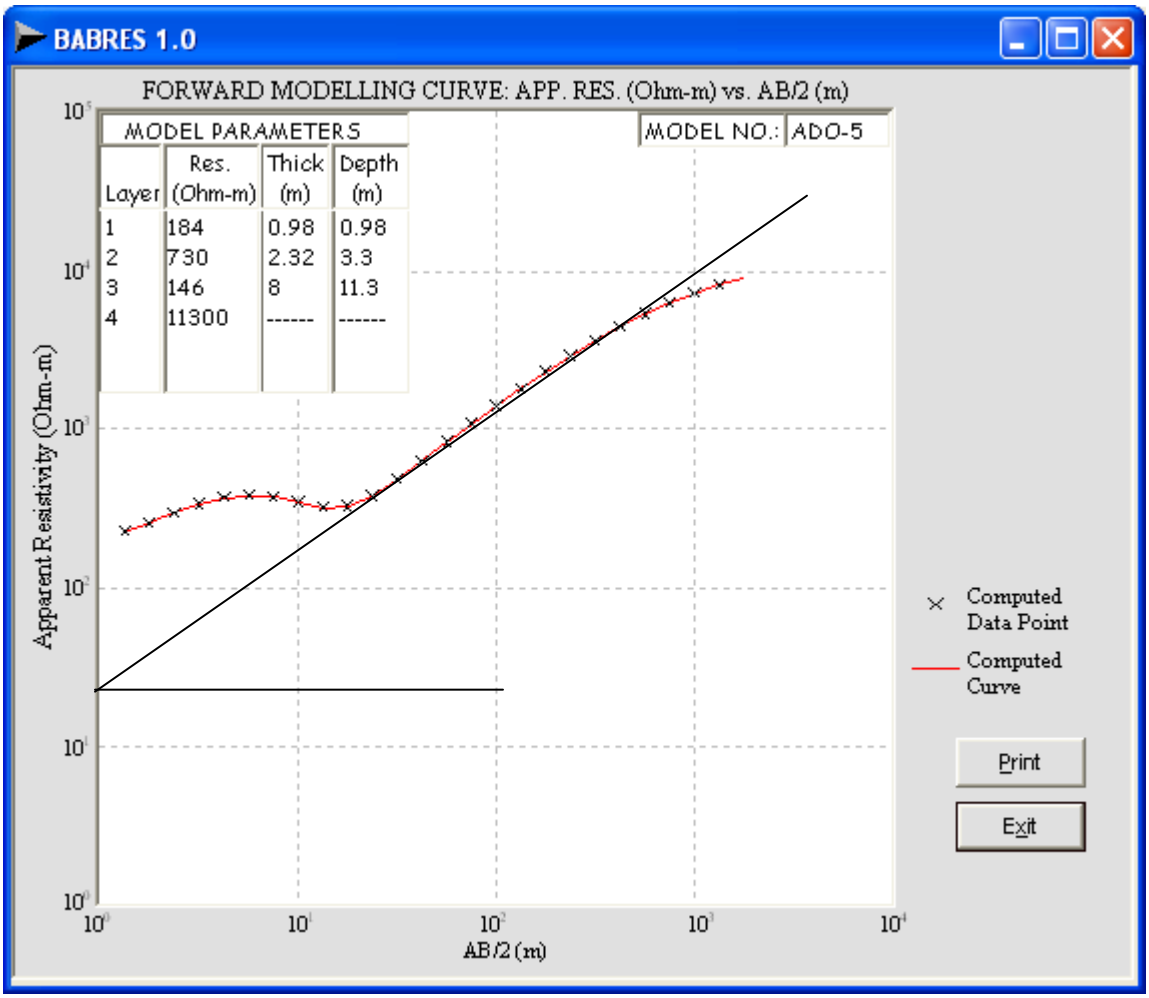

(a) Note: Transition Zone Not Detectable, RR = ?, TR_1 =?, TR_2 = 0.59, dL = 0 , drag angle = 0, γ = 38^0

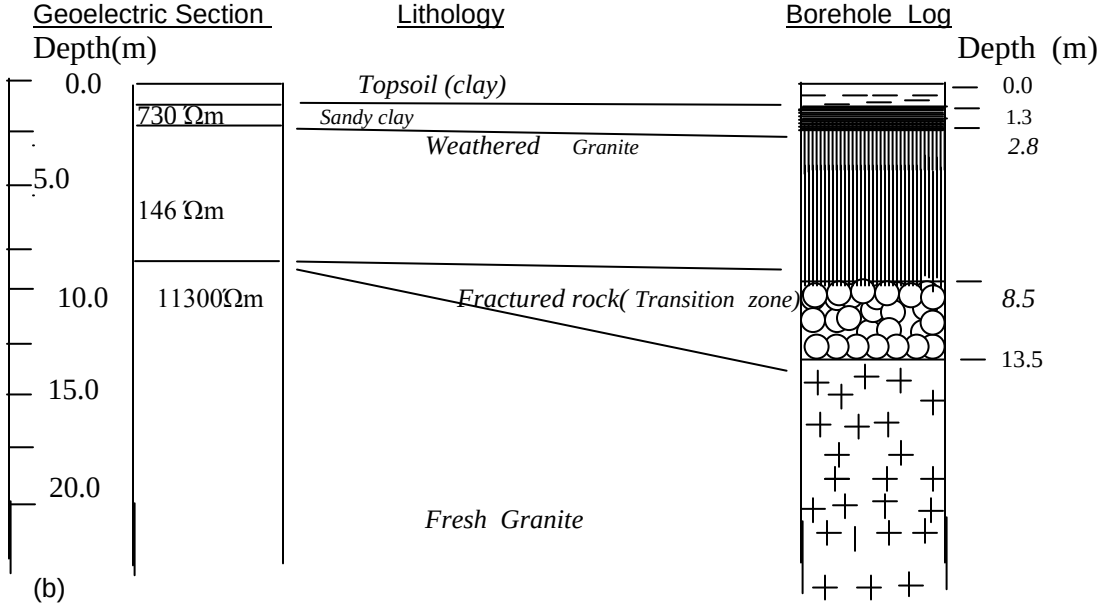

Figure 3: (a) KH- Field Curve V of a drilled Borehole at Ado-Ekiti, Ekiti State.
(b) Lithologic and Geoelectric Section of the Borehole Site.

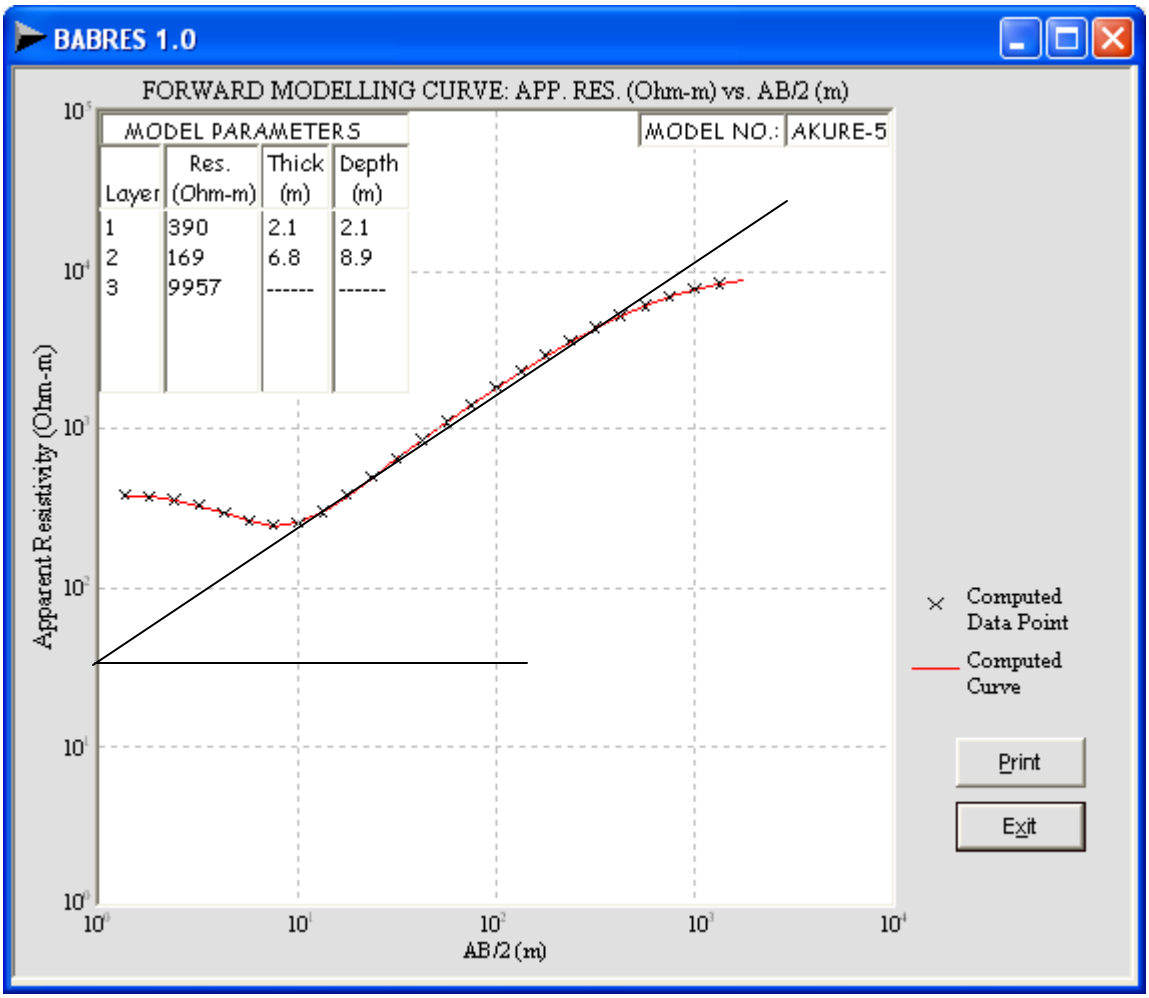

(a) Note: Transition Zone Not Detectable, RR = 0.0, TR_1 =0.0, TR_2 =0.67, dL =0 ,drag angle = 0, γ =38^0

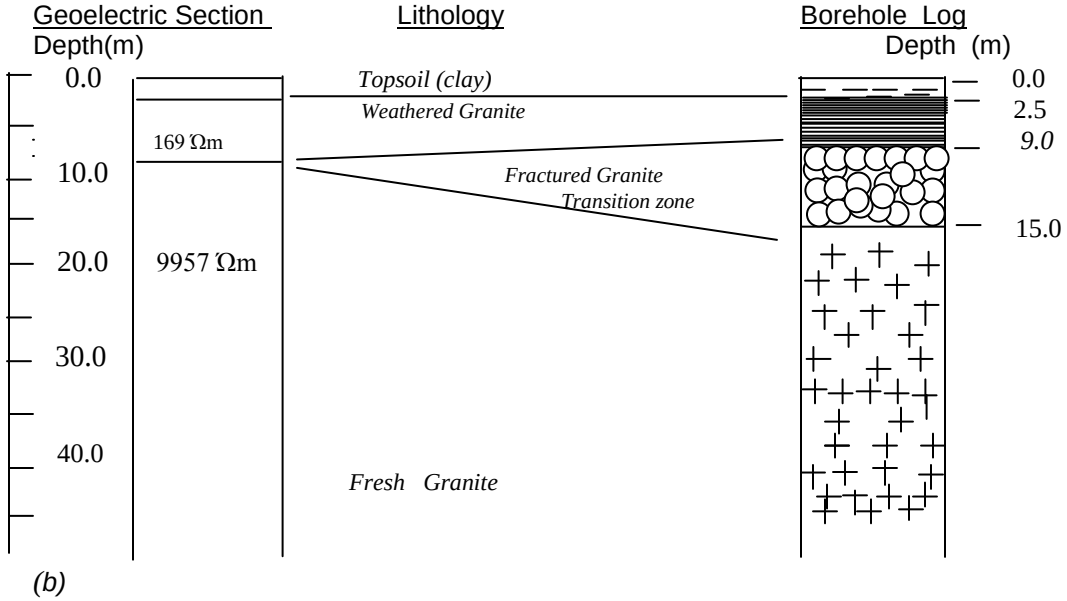

(b)

Figure 4: (a) H- Field Curve V of a Drilled Borehole at Akure, Ondo State.
(b) Lithologic and Geoelectric Section at the Borehole Site.

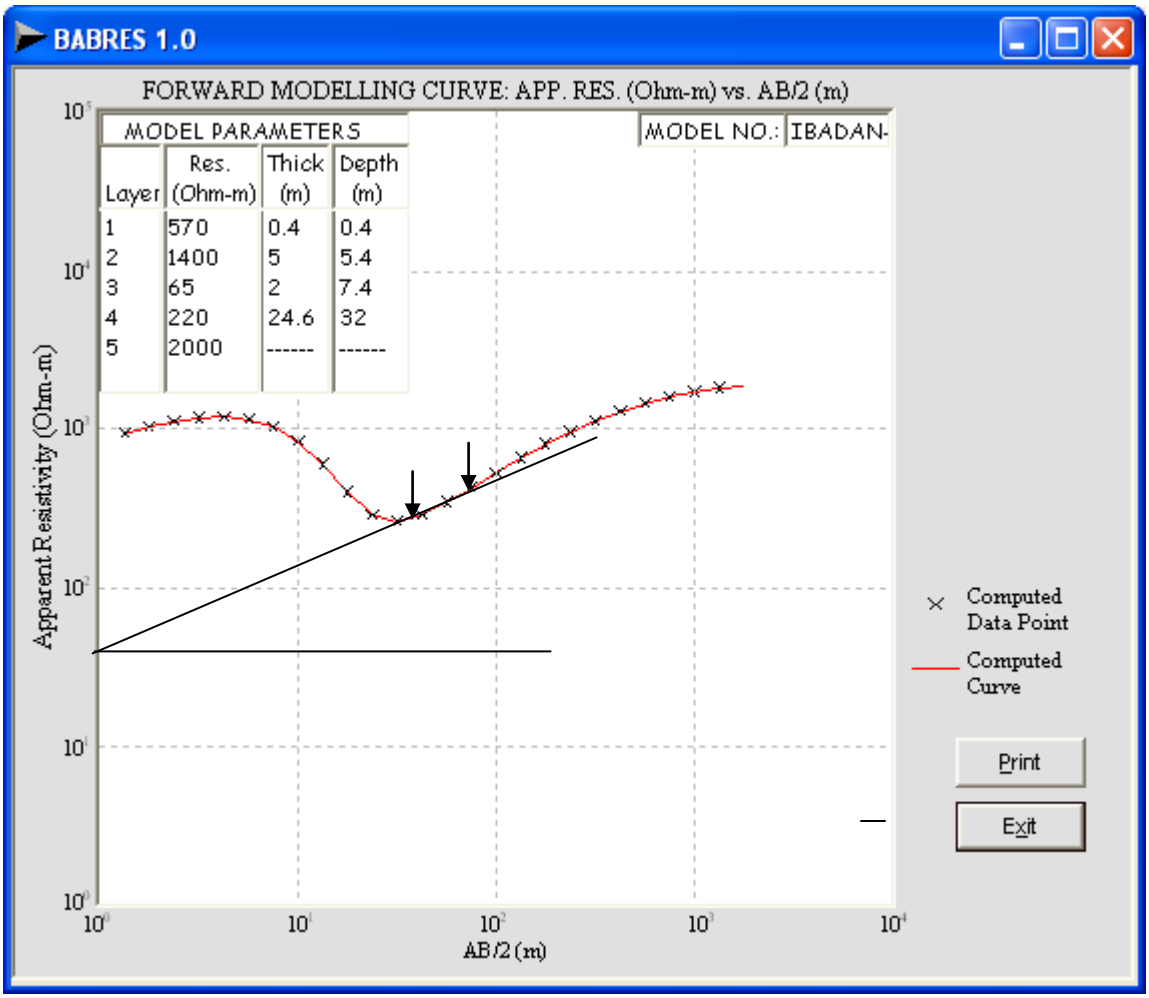

(a) Note: Transition Zone Detectable, RR = 3.38, TR_1 =3.32, TR_2 = 1.53, dL = 0.90cm, drag angle = 23^0

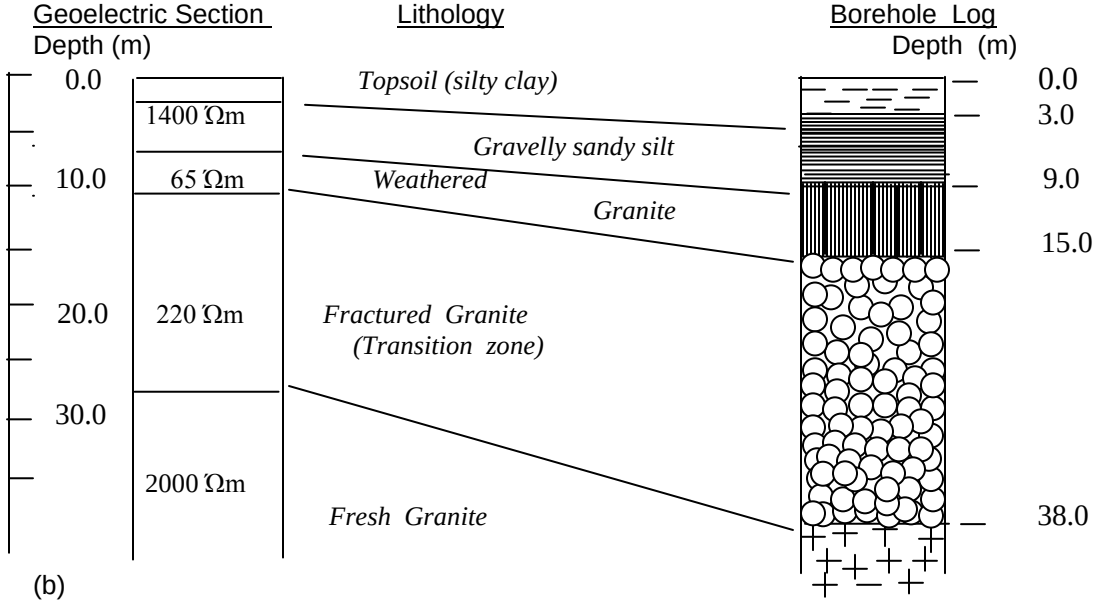

(b)

Figure 5: (a) KHA- Field Curve I of a Drilled Borehole at Ibadan, Oyo State.
(b) Lithologic and Geoelectric Section of the Borehole Site.

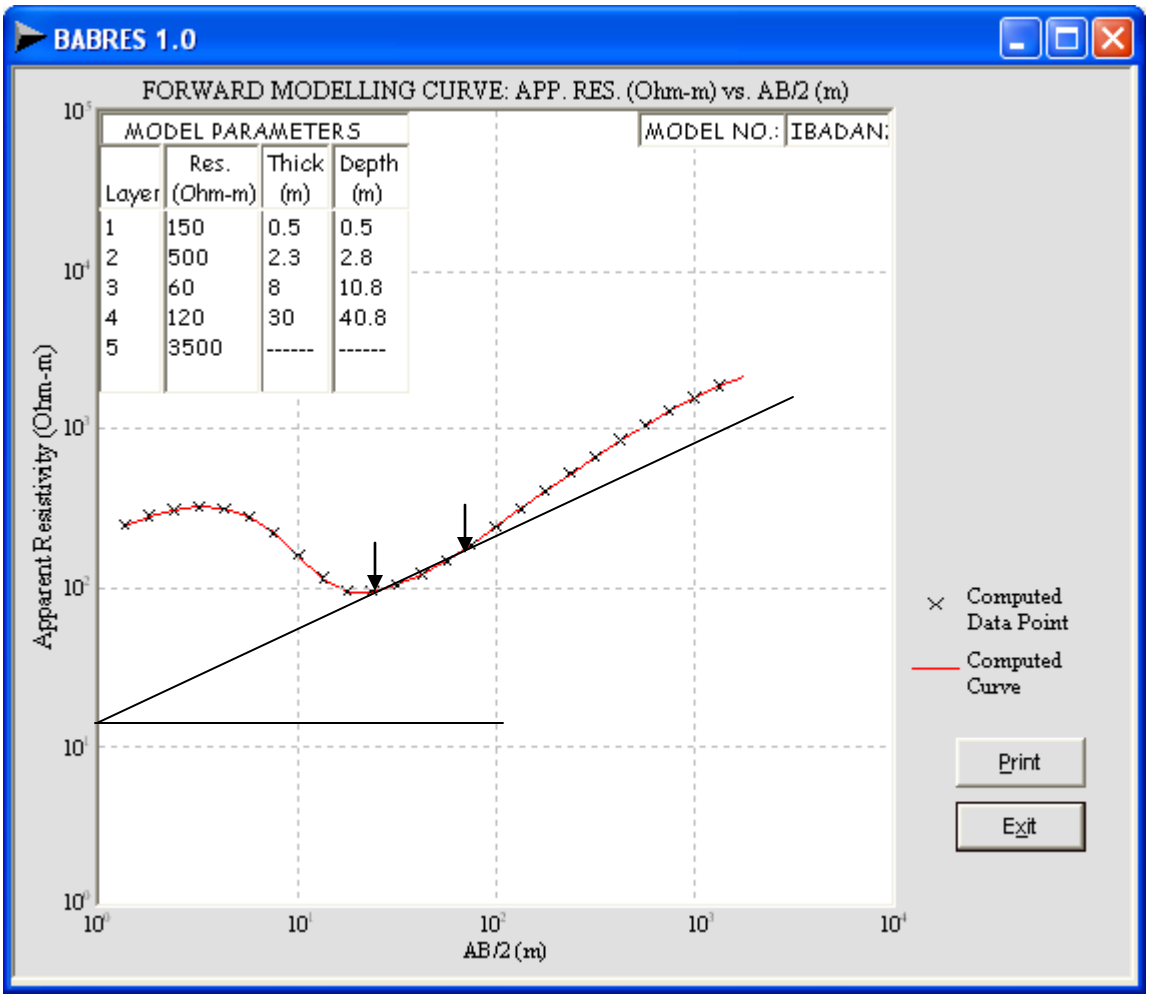

(a) Note: Transition Zone Detectable, RR = 2.00, TR_1 =2.78.32, TR_2 = 1.17, dL = 1.70cm ,drag angle = 22^0

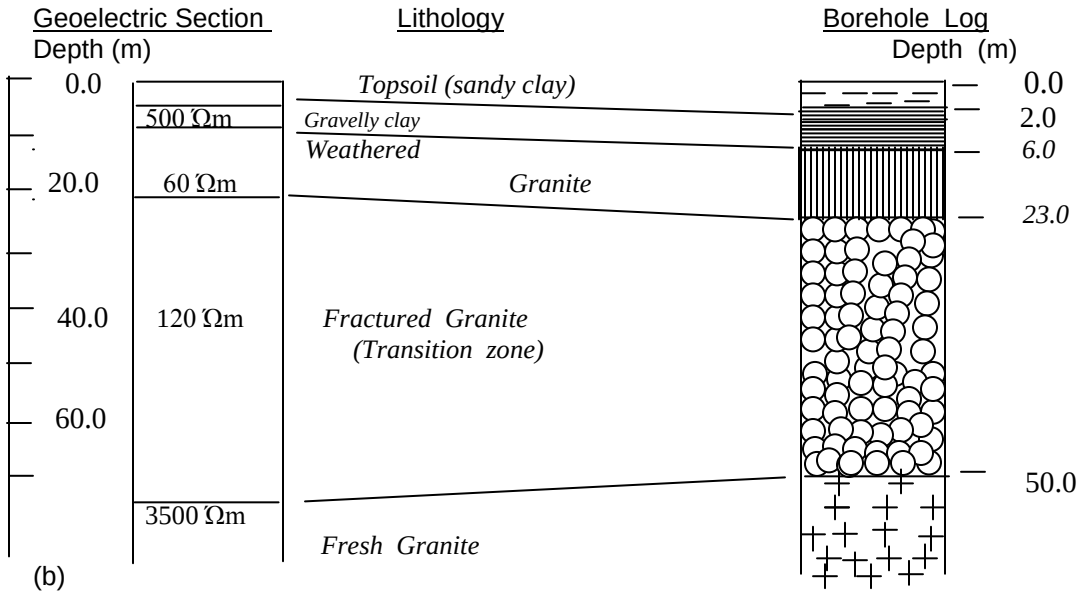

(b)

Figure 6: (a) KHA- Field Curve II of a Drilled Borehole at Ibadan, Oyo State.
(b) Lithologic and Geoelectric Section of the Borehole Site.

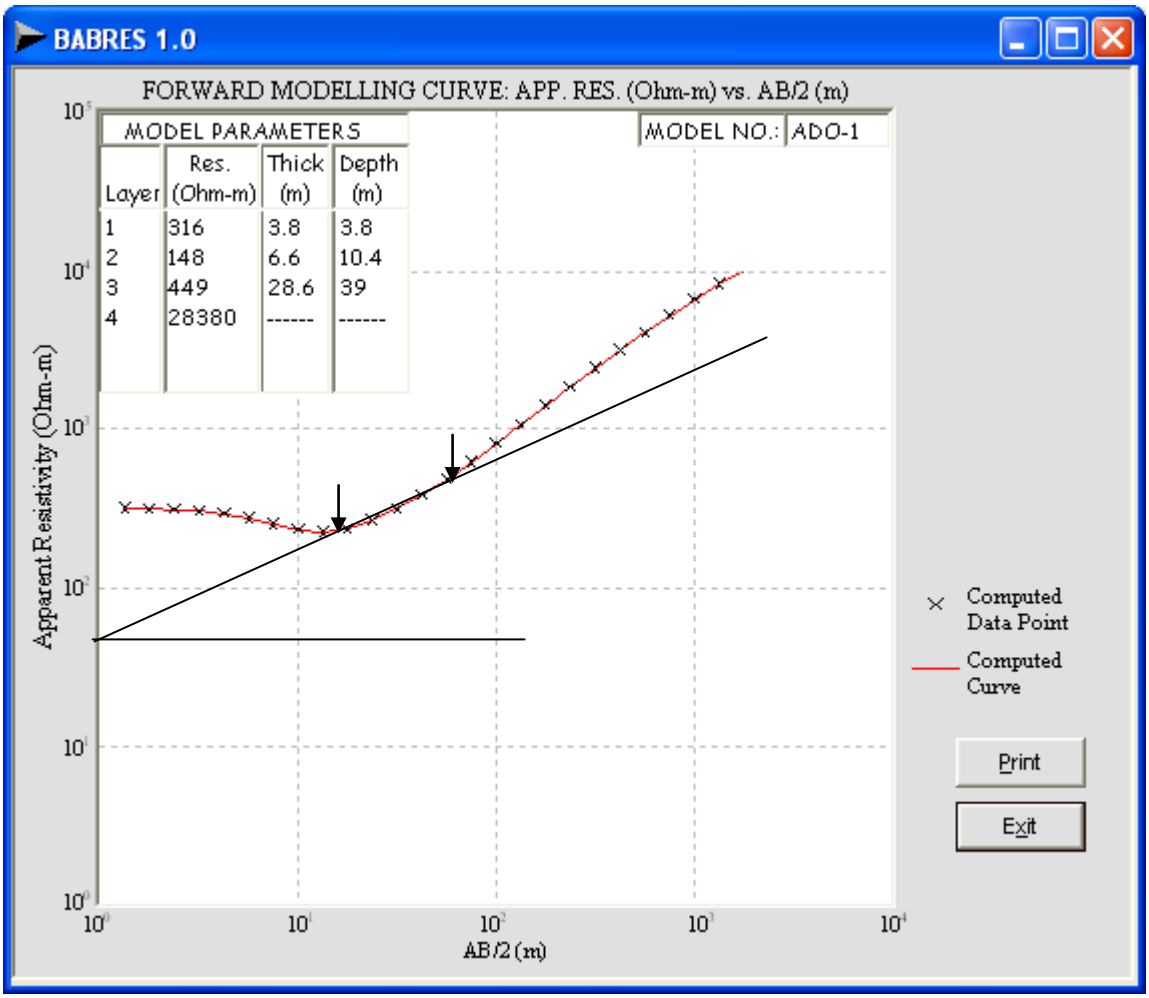

(a) Note: Transition Zone Detectable, RR = 303, TR_1 =2.75, TR_2 =1.10, dL =1.90cm ,drag angle = 23^0

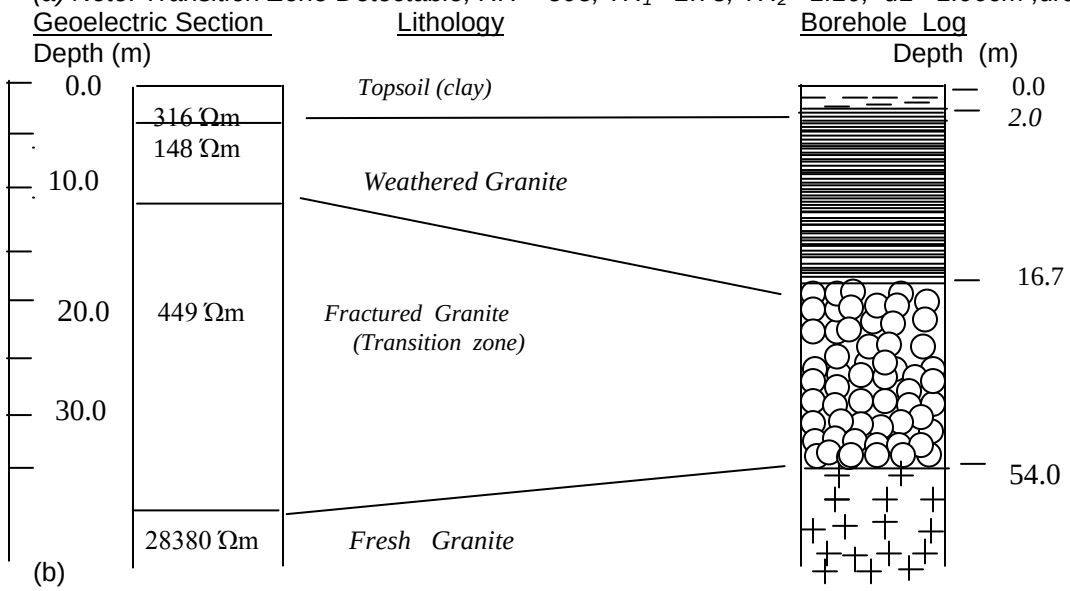

Figure 7: (a) HA- Field Curve I of a Drilled Borehole at Ado-Ekiti, Ekiti State.
(b) Lithologic and Geoelectric Section of the Borehole Site.

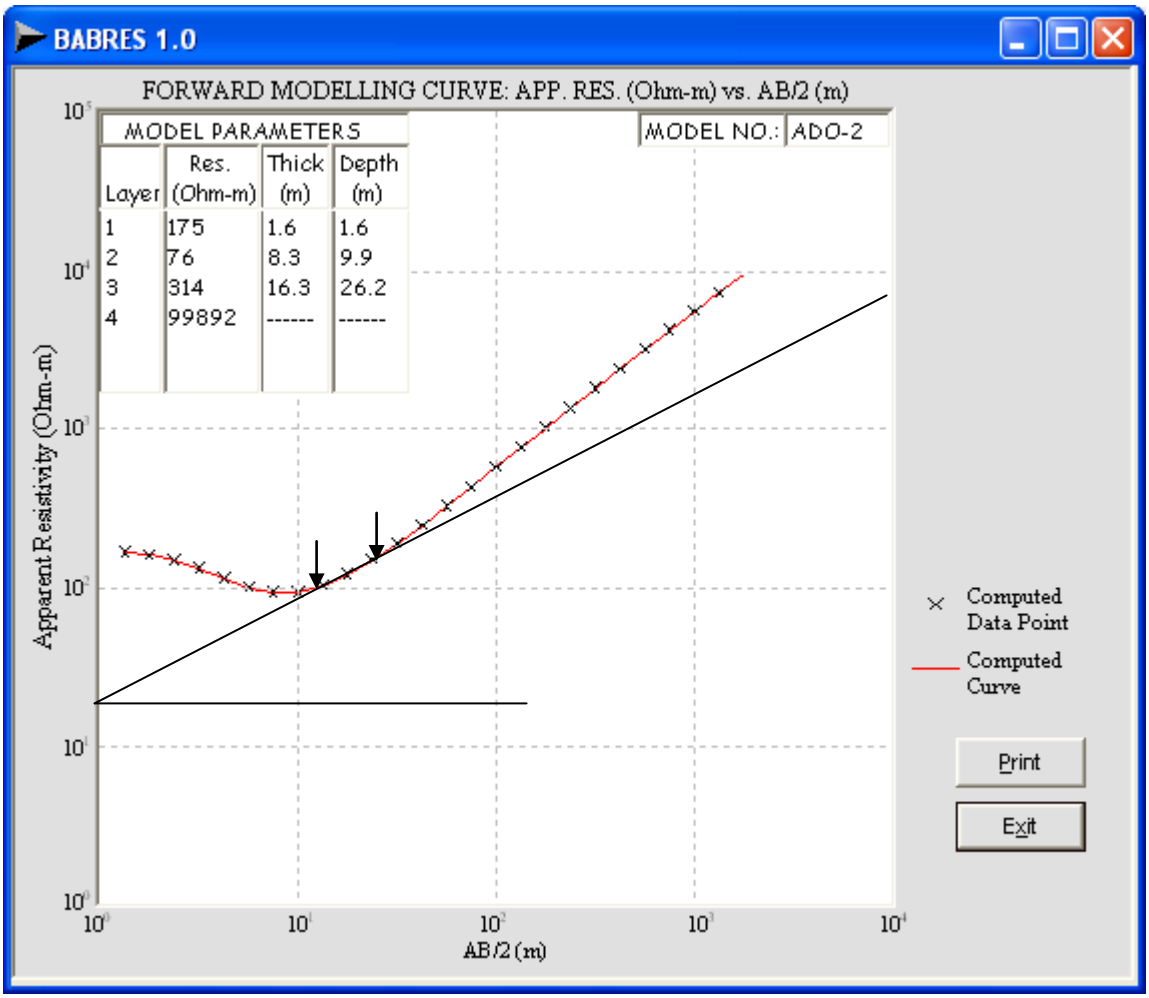

(a) Note: Transition Zone Detectable, RR = 4.13, TR_1 =1.65, TR_2 =2.43, dl =1.00cm ,drag angle = 23^0

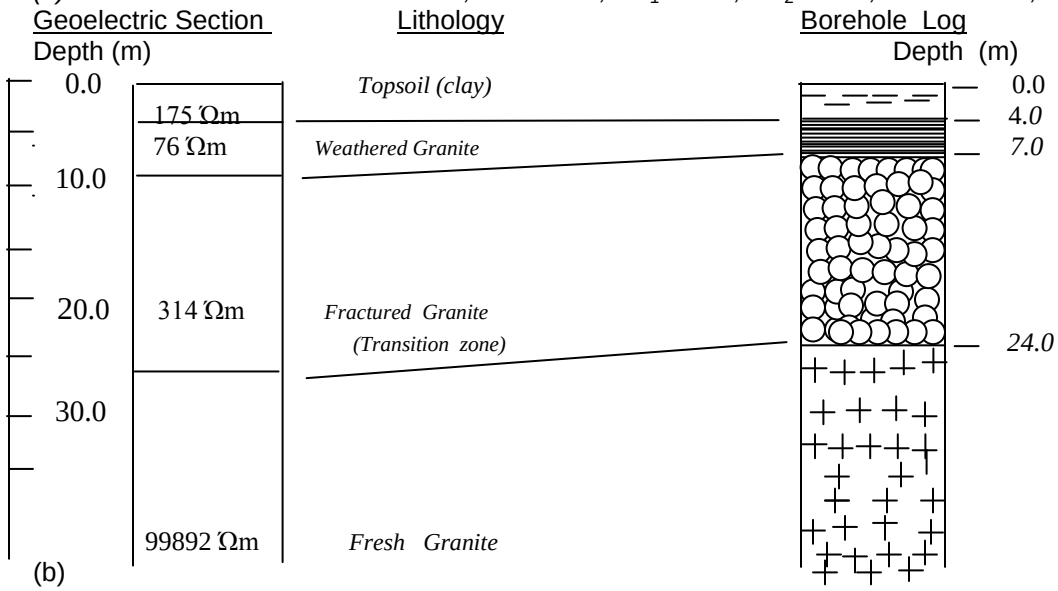

Figure 8: (a) HA- Field Curve II of a Drilled Borehole at Ado-Ekiti, Ekiti State.
(b) Lithologic and Geoelectric Section at the Borehole Site.

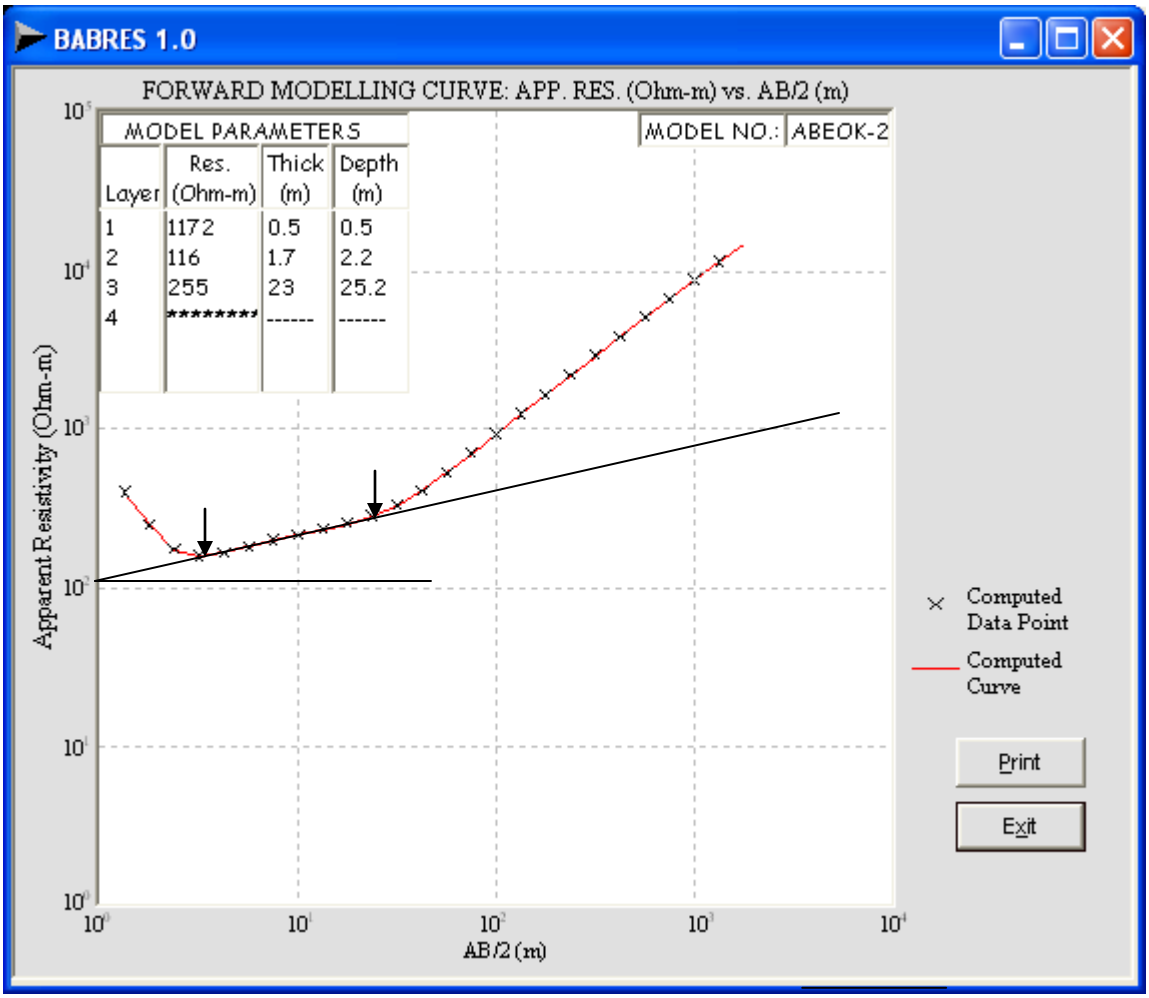

(a) Note: Transition Zone Detectable, RR = 2.20, TR_1 =10.45, TR_2 =3.13, dL =2.60cm ,drag angle = 17^0

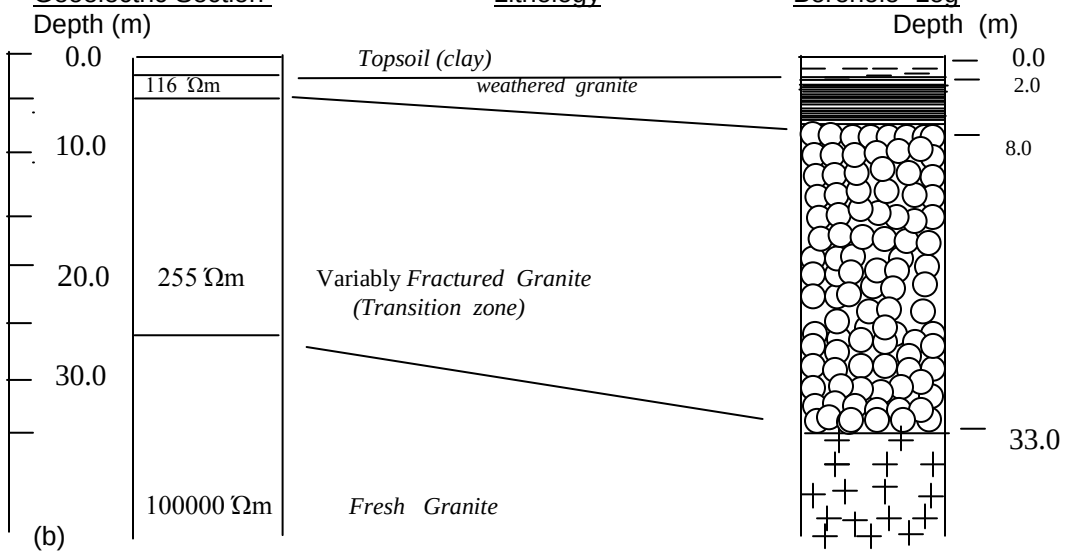

Figure 9: (a) HA- Field Curve II of a Drilled Borehole at Abeokuta, Ogun State.
(b) Lithologic and Geoelectric Section at the Borehole Site.

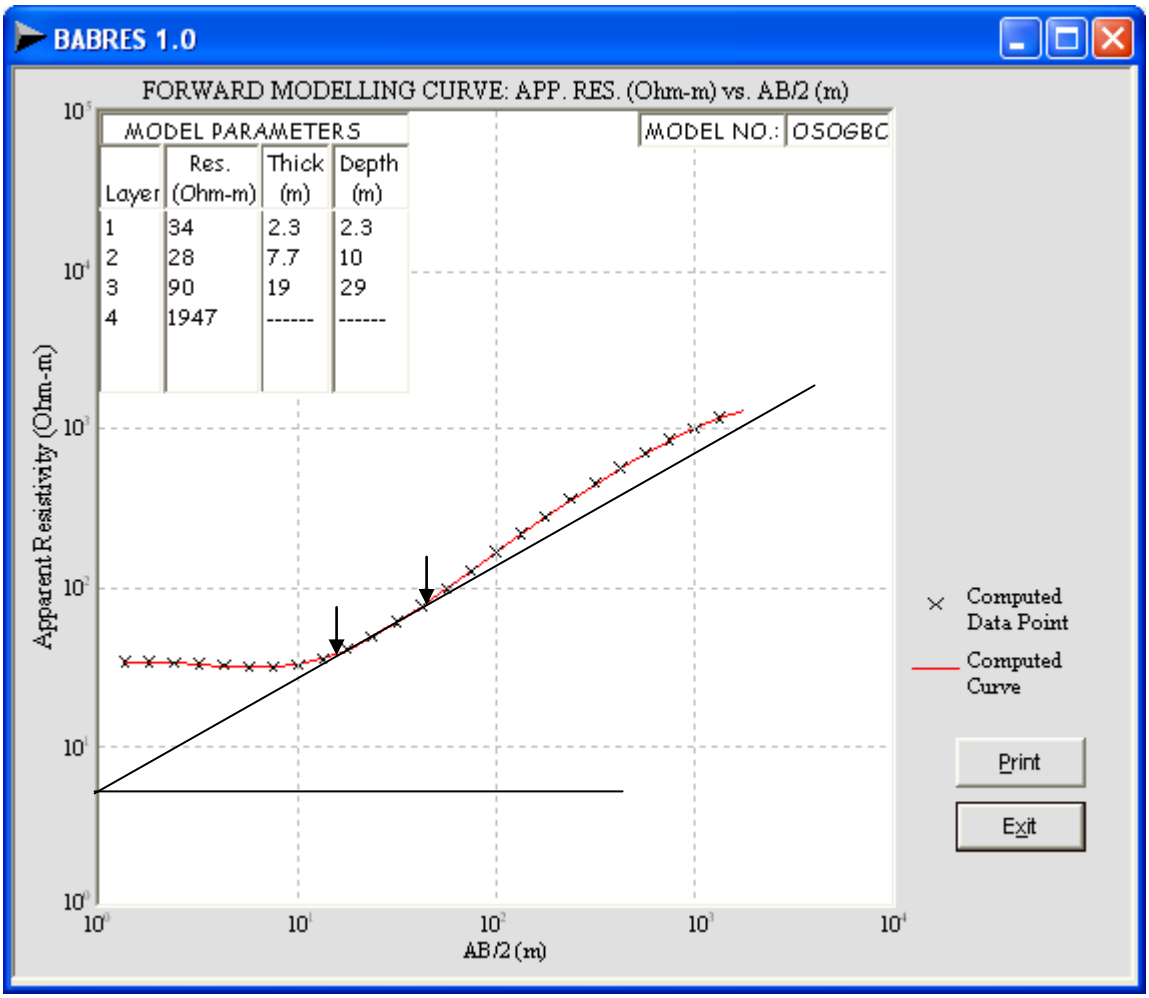

(a) Note: Transition Zone Detectable, RR = 3.21, TR_1 =1.90, TR_2 =1.383, dl =1.50cm ,drag angle = 23^0

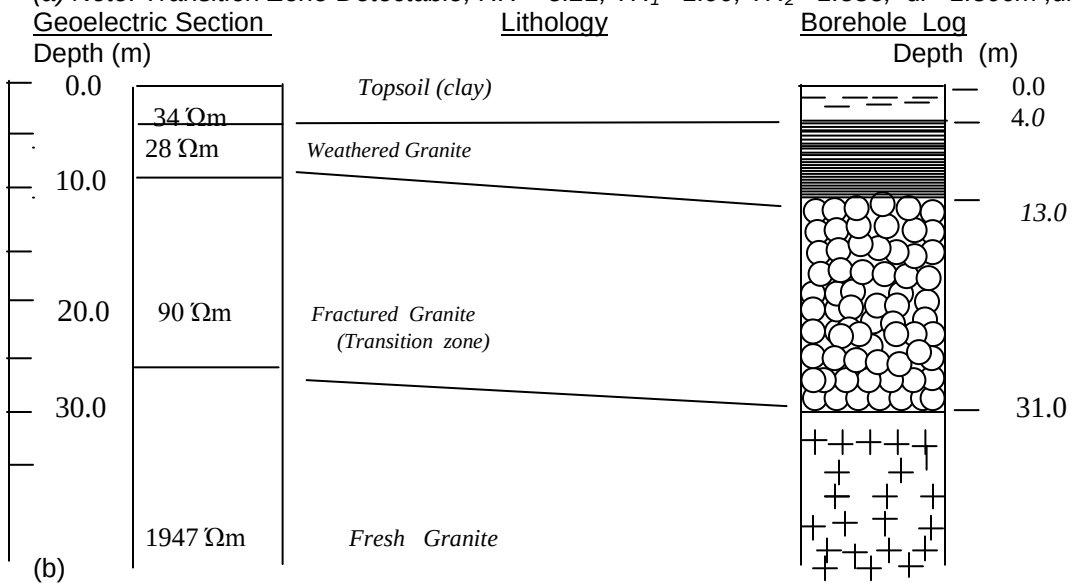

Figure 10: (a) HA- Field Curve II of a Drilled Borehole at Osogbo, Osun State.
(b) Lithologic and Geoelectric Section at the Borehole Site.

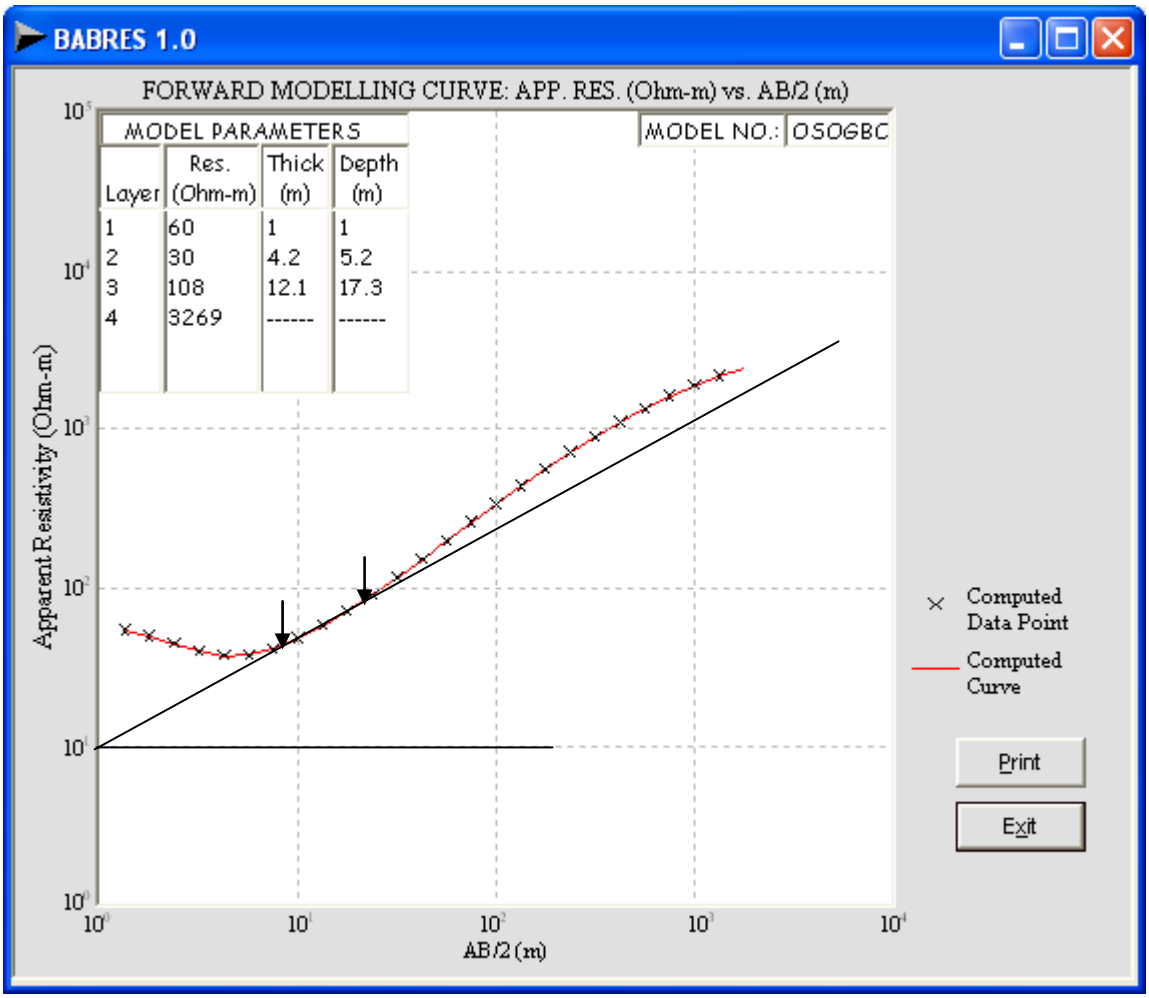

(a) Note: Transition Zone Detectable, RR = 3.60, TR_1 =2.33, TR_2 =1.44, dl =1.40cm ,drag angle = 23^0

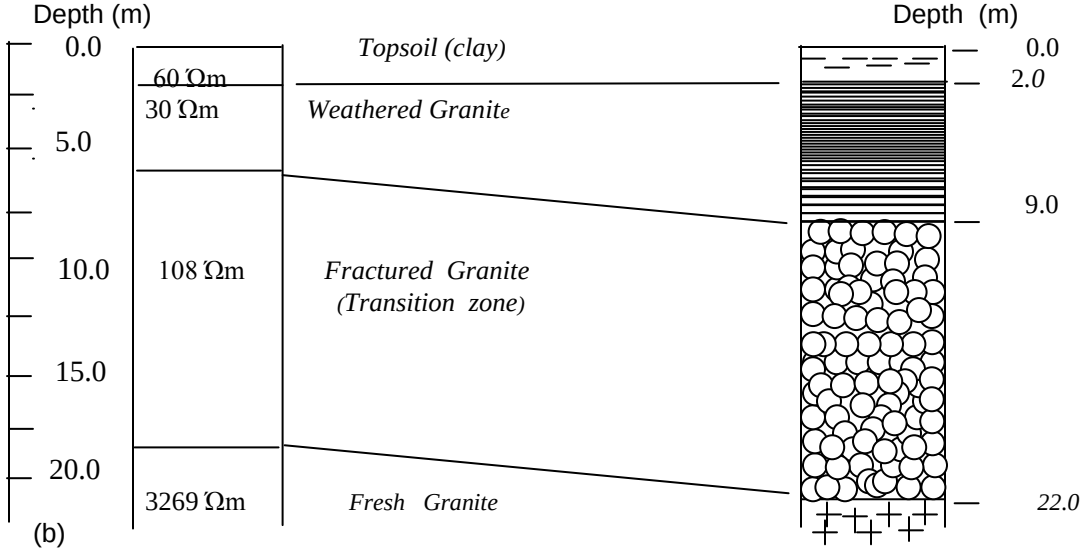

Figure 11: (a) HA- Field Curve III of a Drilled Borehole at Osogbo, Osun State.
(b) Lithologic and Geoelectric Section at the Borehole Site.

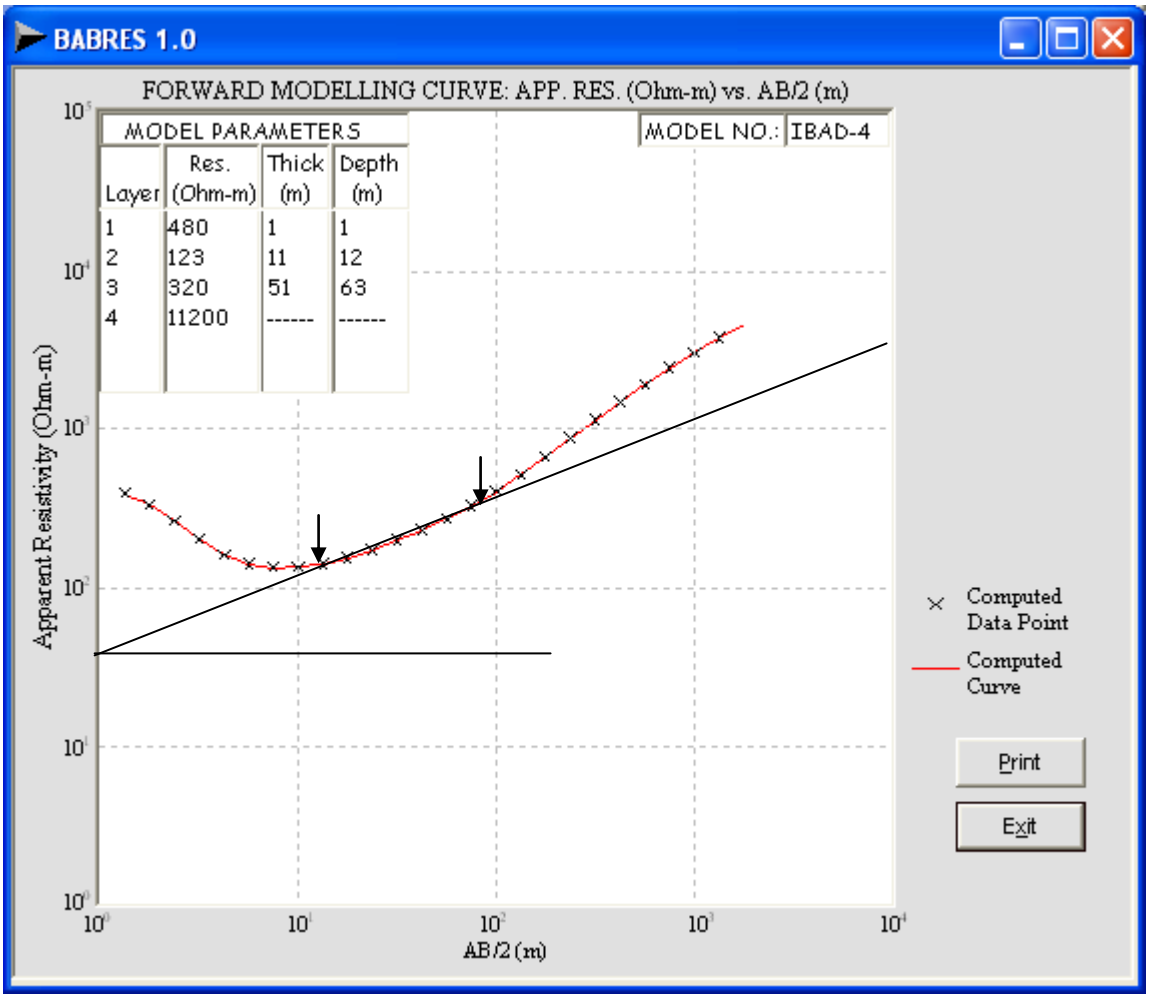

(a) Note: Transition Zone Detectable, RR = 2.60, TR_1 =4.25, TR_2 =3.03, dl = 3.0cm ,drag angle = 21^0

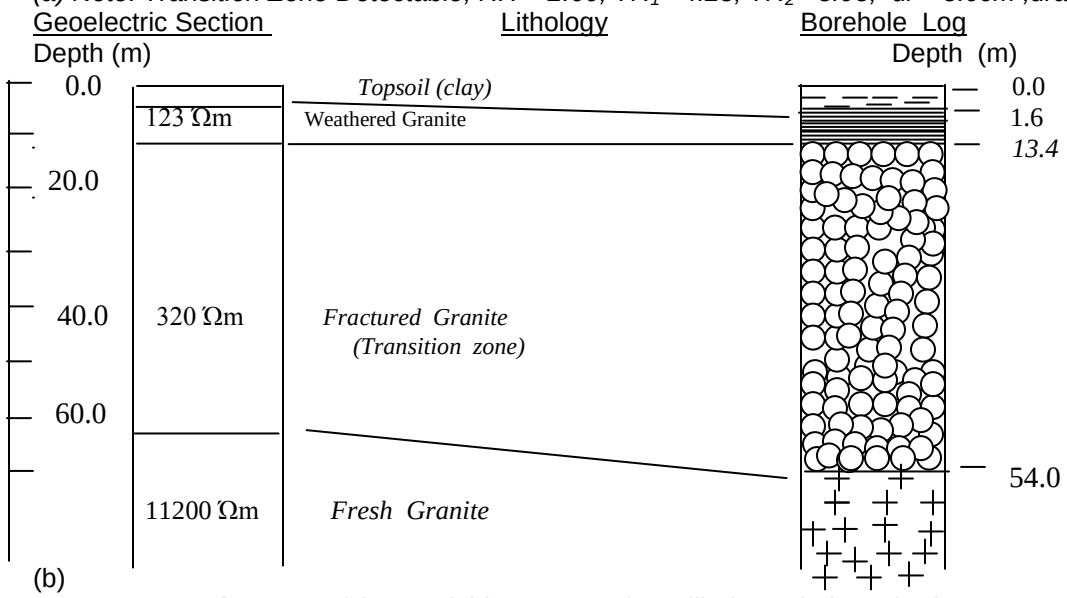

Figure 12: (a) HA- Field Curve IV of a Drilled Borehole at Ibadan, Oyo State.
(b) Lithologic and Geoelectric Section of the Borehole Site.

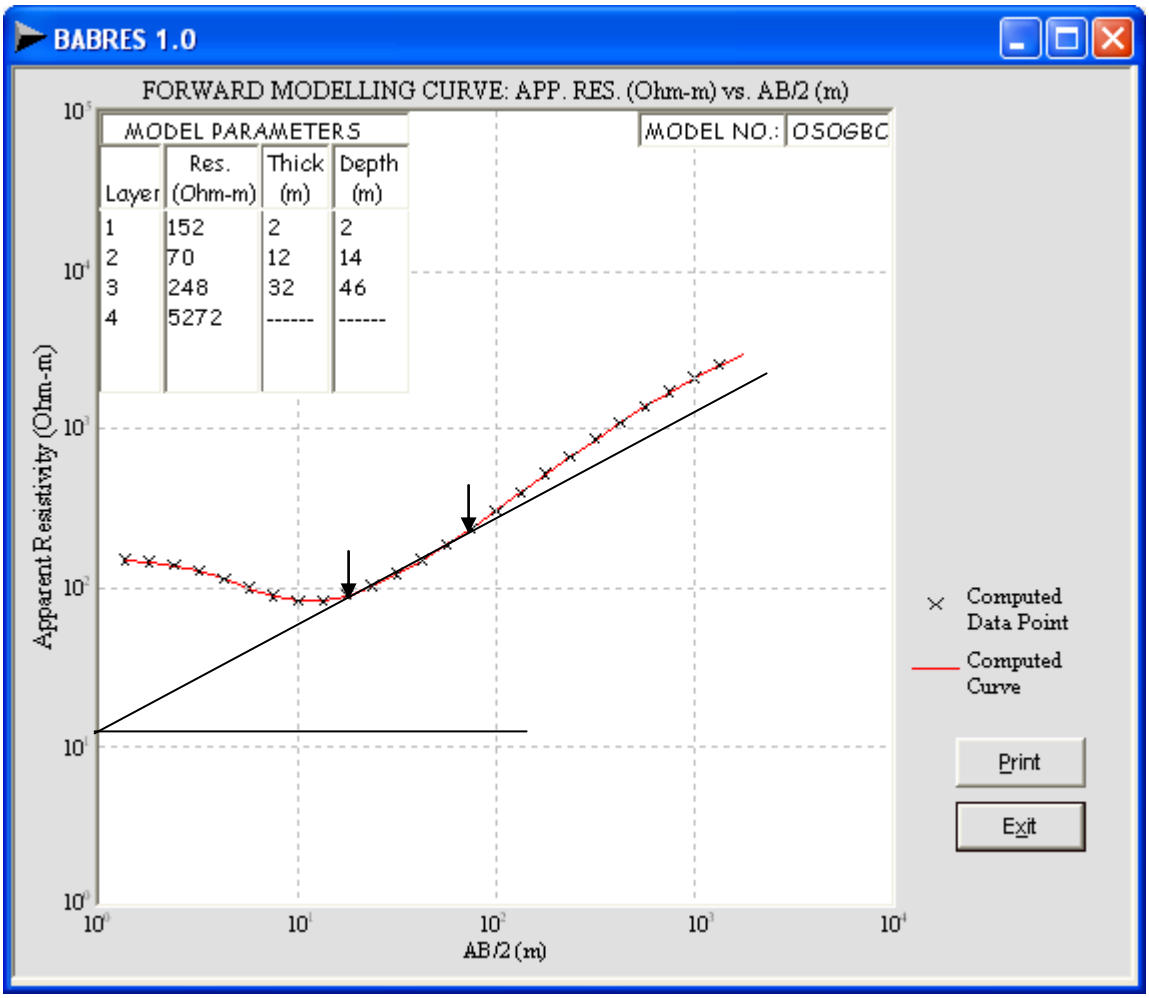

(a) Note: Transition Zone Detectable, RR = 3.54, TR_1 =2.29, TR_2 =1.99, dL =2.10cm , drag angle = 23^0

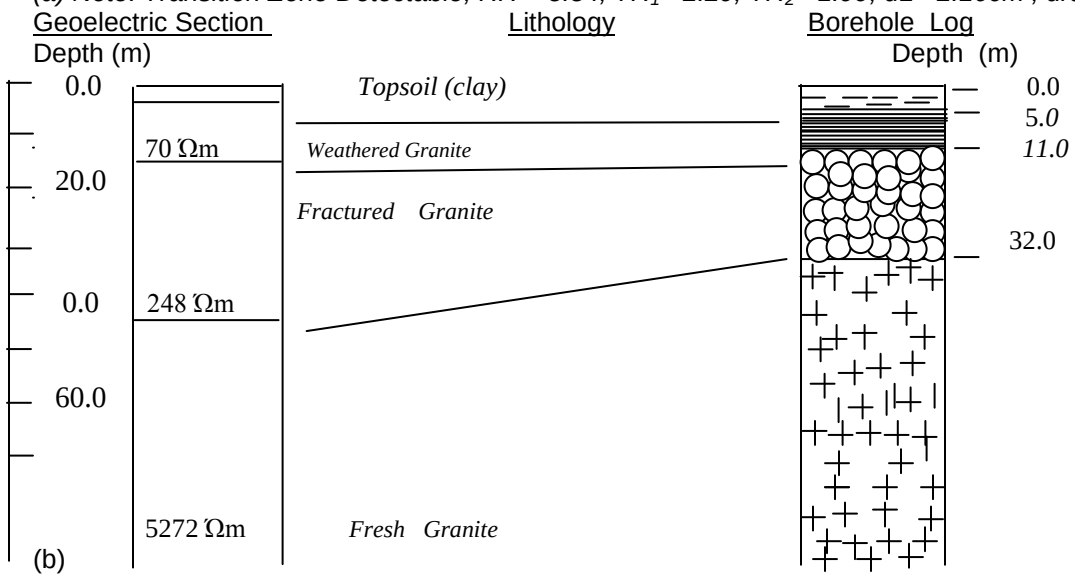

Figure 13: (a) HA- Field Curve I of a Drilled Borehole at Osogbo, Osun State.
(b) Lithologic and Geoelectric Section at the Borehole Site.

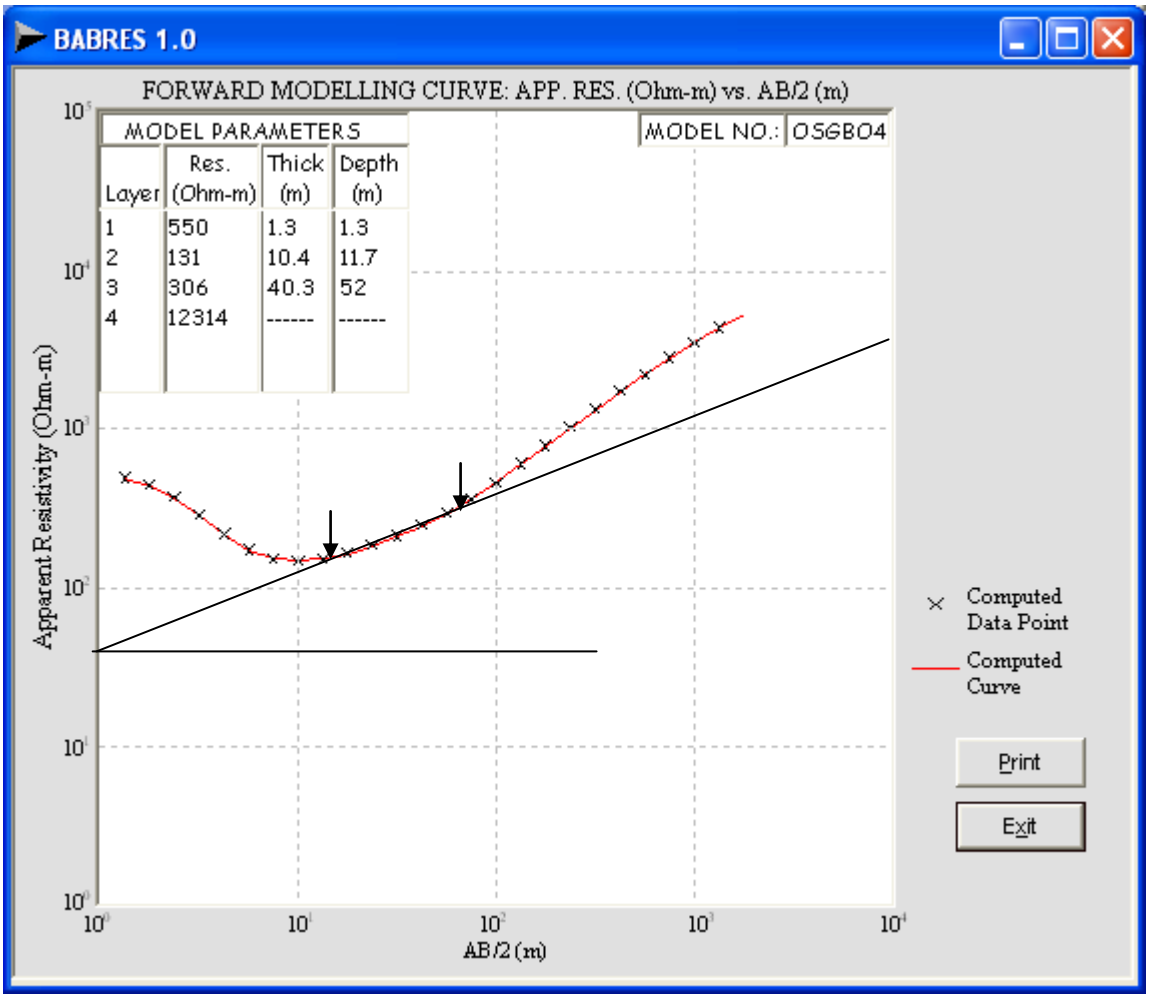

(a) Note: Transition Zone Detectable, RR = 2.34, TR_1 =3.44, TR_2 =3.70 , dL = 2.30 cm ,drag angle = 21^0

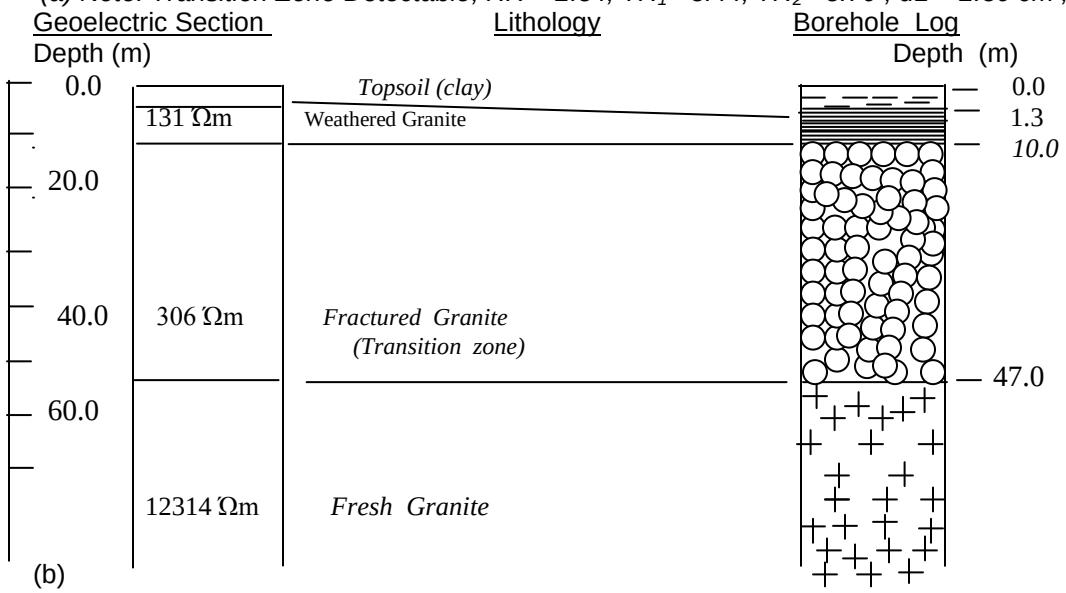

Figure 14: (a). HA- Field Curve IV of a Drilled Borehole at Osogbo, Osun State.
(b) Lithologic and Geoelectric Section of the Borehole Site.

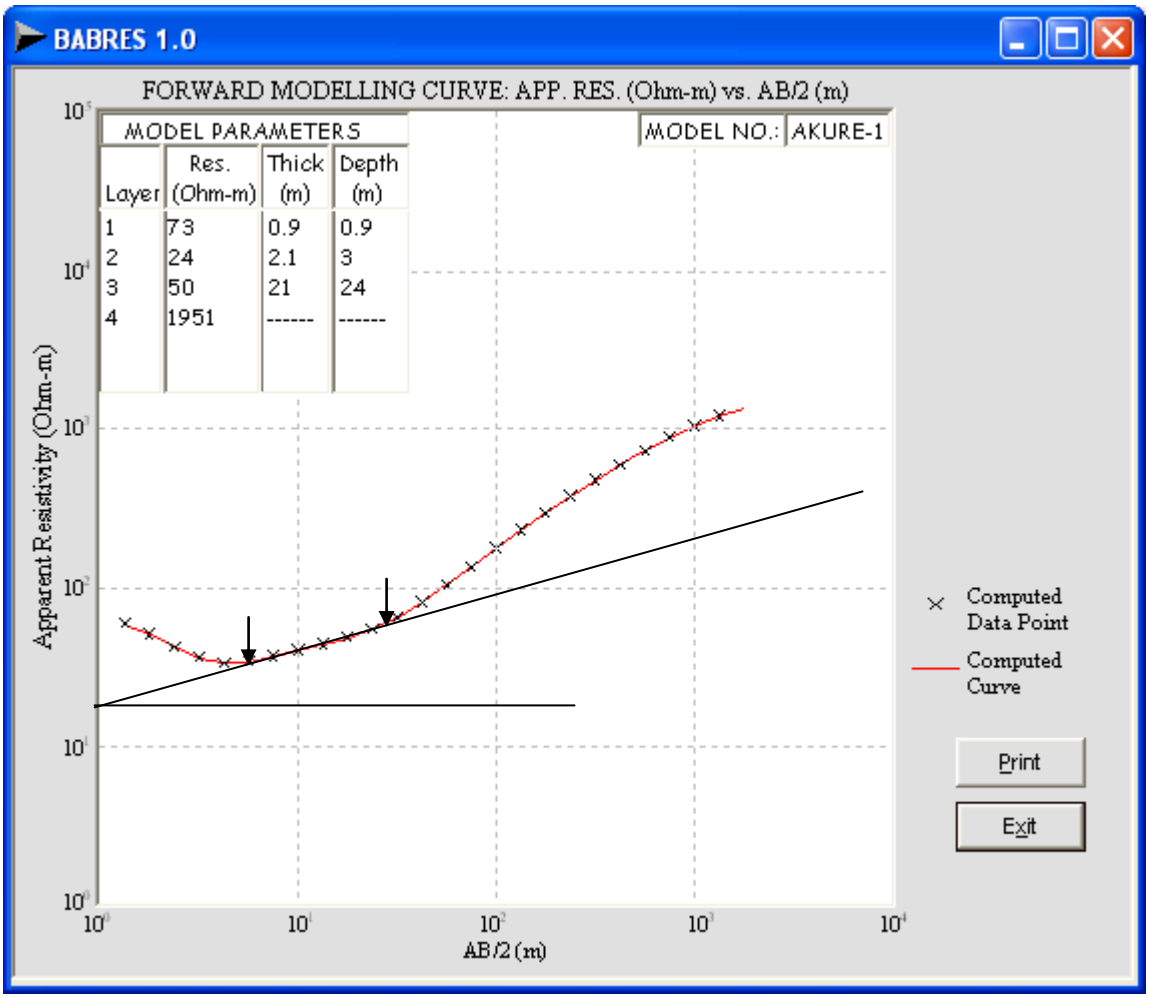

(a) Note: Transition Zone Detectable, RR = 2.08, TR_1 =9.00, TR_2 =2.33, dL =2.45cm ,drag angle = 20^0

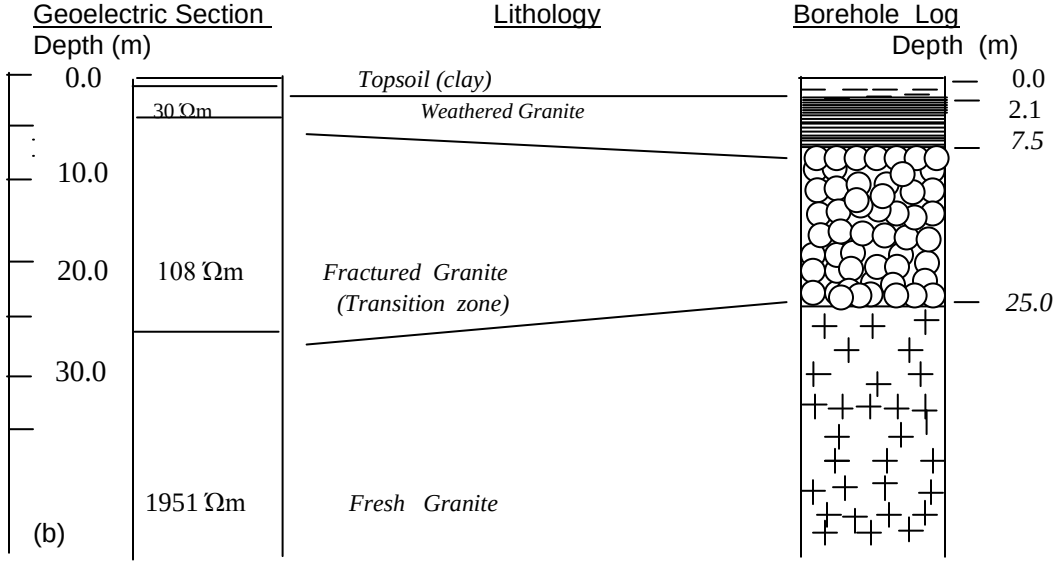

Figure 15: (a) HA- Field Curve I of a Drilled Borehole at Akure, Ondo State.
(b) Lithologic and Geoelectric Section at the Borehole Site.

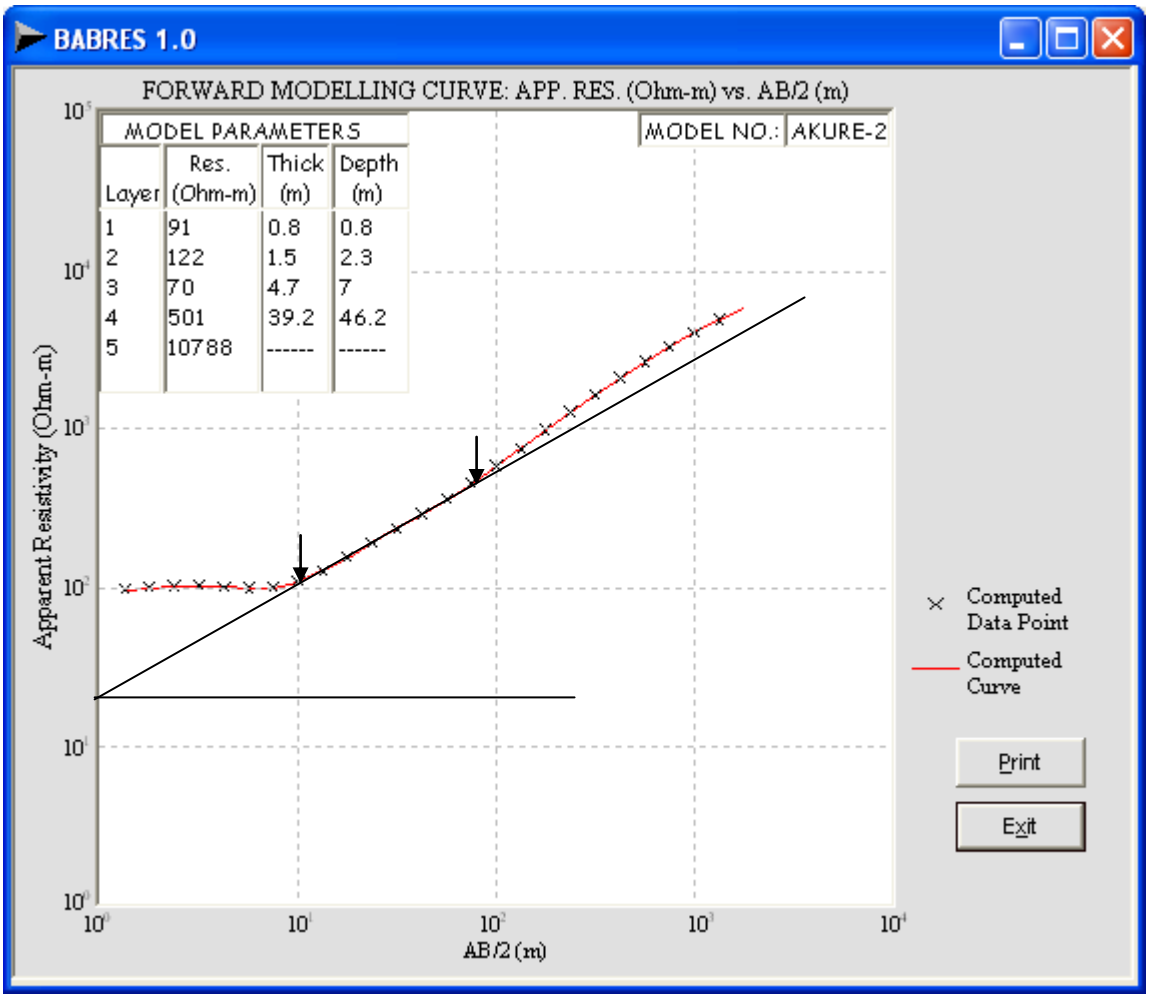

(a) Note: Transition Zone Detectable, RR = 7.16, TR_1 =5.60, TR_2 = 3.00, dL = 3.10 cm ,drag angle = 23^0

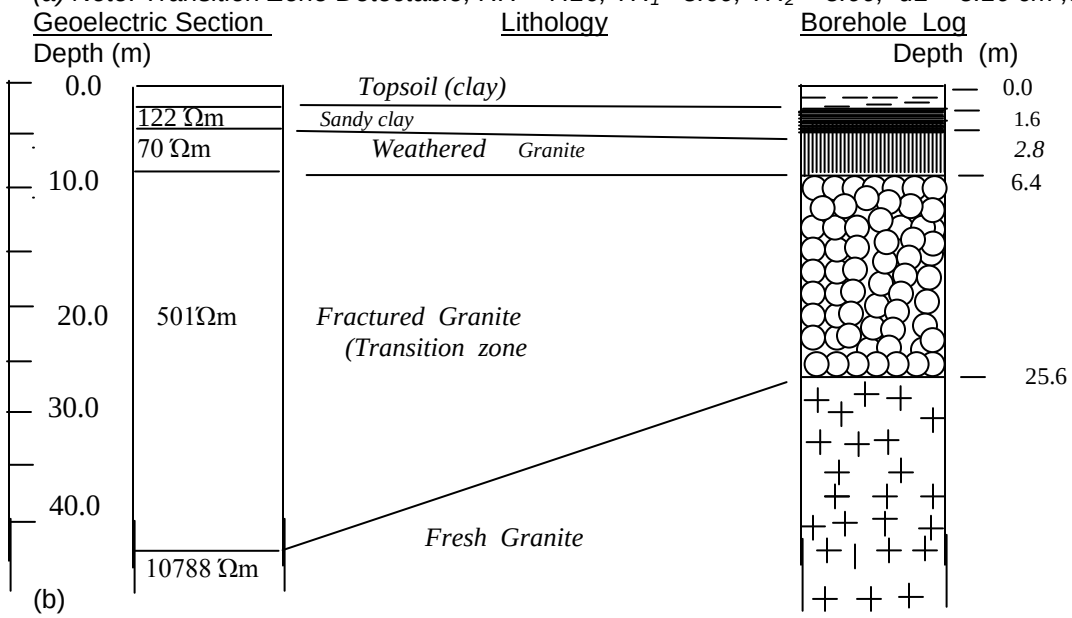

Figure 16: (a) KHA- Field Curve II of a Drilled Borehole at Akure, Ondo State.
(b) Lithologic and Geoelectric Section of the Borehole Site.

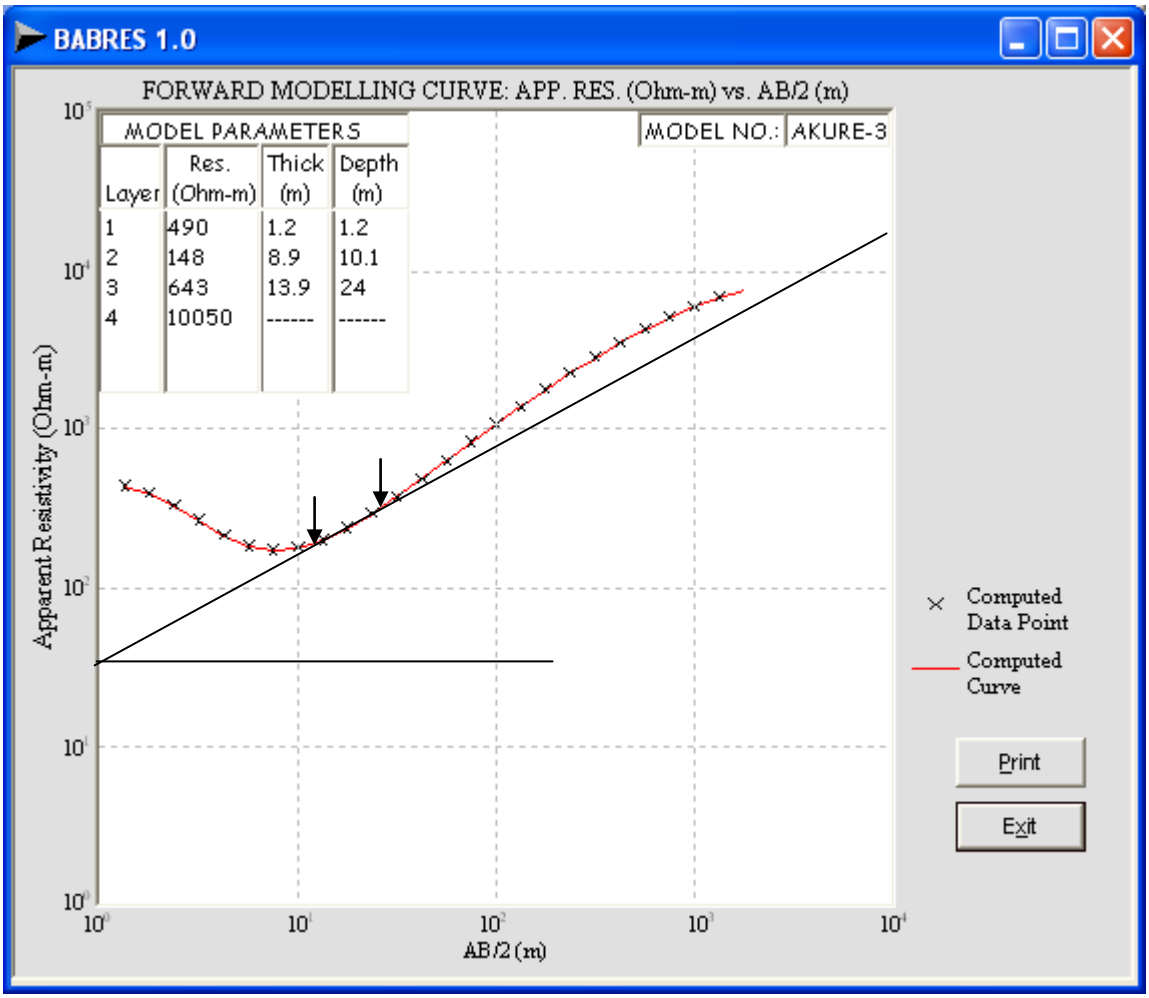

(a) Note: Transition Zone Detectable, RR = 4.34, TR_1 =1.38, TR_2 =1.54, dL =1.10 cm ,drag angle = 23^0

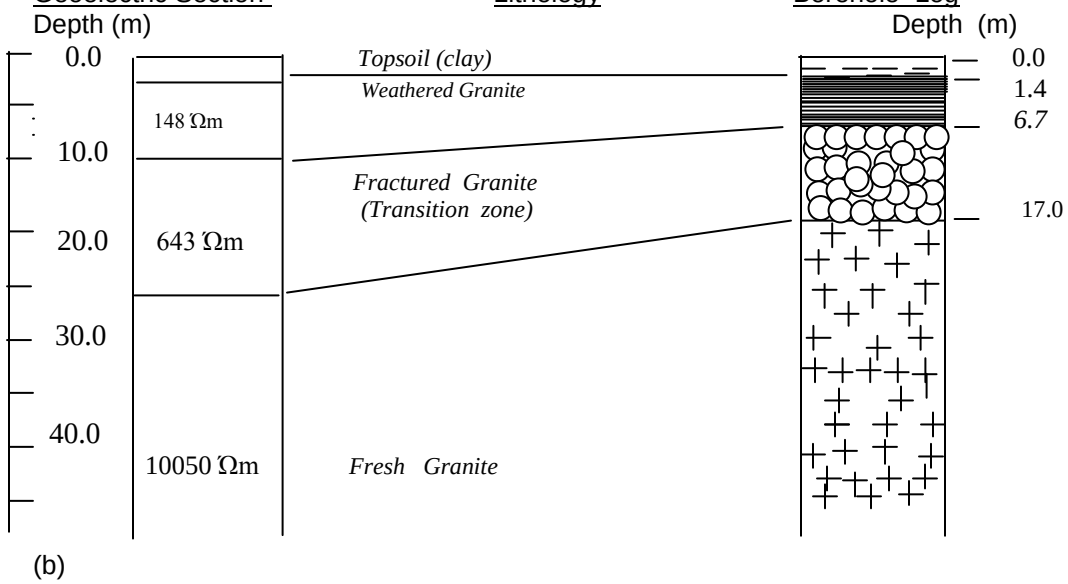

(b)

Figure 17: (a) HA- Field Curve III of a Drilled Borehole at Akure, Ondo State.
(b) Lithologic and Geoelectric Section at the Borehole Site.

Table 2: Summary of VES and Lithologic Log Records and Parameters.

S/No	Location	Resistivity. Ratio (RR)	Thickness. Ratio I (TR1)	Thickness Ratio II (TR2)	Drag Length DL (cm)	B^0	γ	Field Curve type	Remarks
1	Ado-Ekiti 5	-	-	0.59	0.0	0	38	KH-	ND
2	Akure 5	-	-	0.67	0.0	0	38	H-	ND
3	Akure 1	2.08	9.00	2.33	2.45	20	-	HA	D
4	Ibadan 2	2.00	2.78	1.17	1.70	22	-	KHA-	D
5	Abeokuta	2.20	10.45	3.13	2.60	17	-	HA-	D
6	Ibadan 4	2.60	4.25	3.03	3.0	21	-	HA	D
7	Osogbo 4	2.34	3.44	3.70	2.30	21	-	HA	D
8	Ado – Ekiti 1	3.03	2.75	1.10	1.90	23	-	HA	D
9	Osogbo 2	3.21	1.90	1.38	1.50	23	-	HA	D
10	Osogbo 1	3.54	2.29	1.99	2.10	23	-	HA-	D
11	Osogbo 3	3.60	2.33	1.44	1.40	23	-	HA	D
12	Ibadan 1	3.38	3.32	1.53	0.90	23	-	KHA-	D
13	Ado – Ekiti 2	4.13	1.65	2.43	1.00	23	-	HA-	D
14	Akure 3	4.34	1.38	1.54	1.10	23	-	HA	D
15	Akure 2	7.16	5.60	3.00	3.10	23	-	KHA-	D

D = Transition zone detectable , ND = Zone not detectable , RR = Resistivity ratio TR1 = Thickness ratio obtained from VES , TR2 = Thickness ratio obtained from lithologic logs

An increase beyond the upper limit in resistivity ratio would lead to a decrease in drag length and finally leads to undetectability of the zone on the VES curve because, the resistivity reflection coefficient (k) between the transition zone and the underlying fresh bedrock approaches +1, which makes differentiation of the zone from the fresh bedrock difficult.

However, it must be stated that, for the zone to be detectable within the resistivity ratio ranges stated above, the corresponding thickness ratios (TR1 or H'/H) must not fall below the limits specified earlier (i.e., 0.73 for the HA- and 1.10 for the KHA- type curves). Figures 3 and 4 present the cases where the thickness ratio requirements are not met, hence the transition zone signatures were not detectable on the VES curve. The inference from these is that while the thickness ratio is independent of the resistivity ratio within the specified limits, the reverse is the case for the resistivity ratio limits as they are valid only for corresponding values of thickness ratios not below the minimum limits (i.e., 0.73 for HA-, and 1.10 for KHA-type curves). From the foregoing, it could therefore be concluded that the transition zone can be identified on the VES curve when the ratio of the thickness of the zone to that of the overlying layers is not less than 0.73 for the HA- and 1.11 for the KHA-type curves Also the resistivity ratio of the zone to that of the immediately overlying weathered layer must range from 1.67 to 4.33 for the HA- and 1.67 to 5.00 for the KHA-type curves. Above these ranges, the zone becomes difficult to differentiate from the fresh basement. Also, while the resistivity ratio limits depend on the minimum thickness ratio requirements for it's validity, the thickness ratio is valid for all resistivity ratios .However, for optimum detectability, the resistivity ratio should be between 3.0 and 3.67 for the HA-type curve and 3.8 – 4.50 for the KHA-type curve.

CONCLUSION

In a typical basement complex environment, the transition zone (saprock) has been identified as a very important lithologic unit whose significance spans through several spheres of endeavors, from groundwater/hydrogeology to engineering foundations design and construction to mention a few.

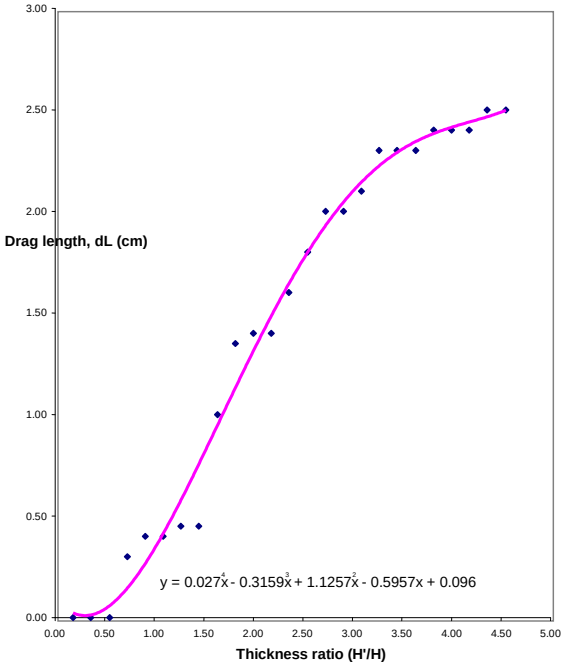

Figure 18: Graph of Drag Length against Thickness Ratio for HA-type Curve (culled from Ademilua, 2007).

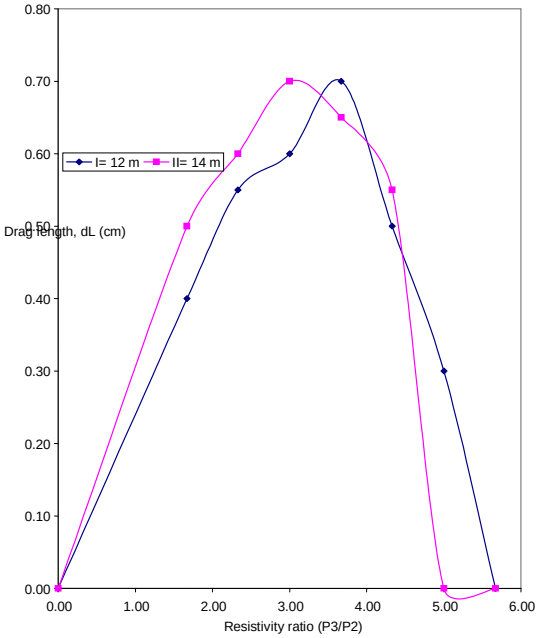

Figure 20: Graph of Drag Length against Resistivity Ratio for HA-type Curve (culled from Ademilua, 2007)

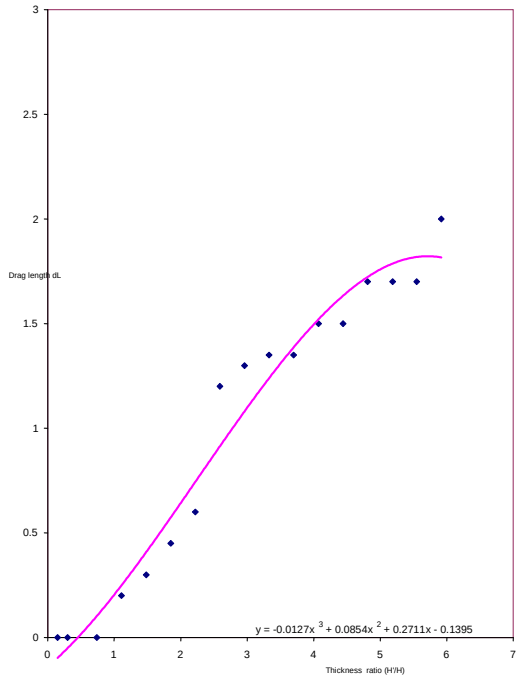

Figure 19: Graph of Drag Length against Thickness Ratio for KHA-type Curve.

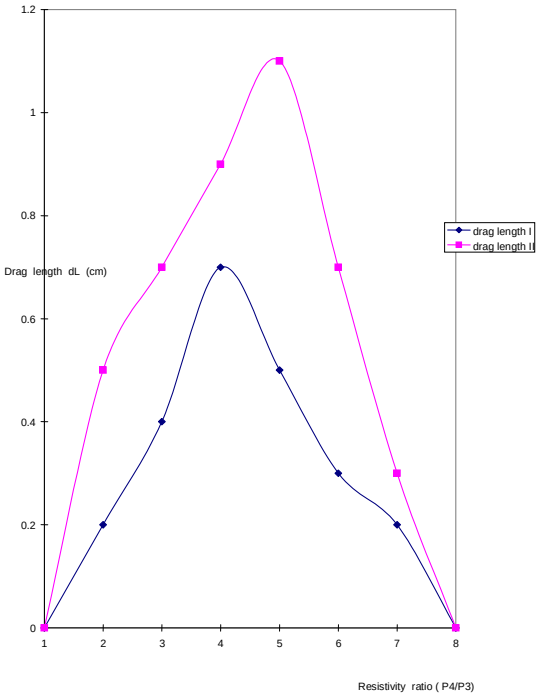

Figure 21: Graph of Drag Length against Resistivity Ratio for KHA-type Curve (culled from Ademilua, 2007).

But in the basement complex rocks of Southwest Nigeria, this horizon which is located between the weathered basement (saprolite) layer and the underlying fresh basement has the tendency to be suppressed on the VES curve.

This transition zone manifests as a drag along the rising segment of an HA-curve or curves ending with HA-. Where this drag is noticeable, the curve is correctly interpreted as a four-layer HA-type curve. However, where the reverse is the case and in which case, the drag becomes undetectable, the curve is inadvertently and incorrectly interpreted as a three-layer H-type curve, or in the case of the five-layer KHA-, as a four-layer KH- type curve, thus resulting in a serious interpretation problem, since subsequent actions supposedly on the interpretation would be based on this faulty premise.

The research approach adopted has been to use fifteen VES datasets obtained from locations that have been drilled and with accompanying borehole driller's logs. The resulting parameters from the analyses of the VES and borehole records were used as field test for the observations and results from the two earlier model approaches. In carrying out the analyses, the field VES data were plotted into field sounding curves using the developed forward modeling software BABRES 1.0. The curves, as usual, were studied for signatures of the transition zone. The drag lengths were measured and recorded for curves displaying evidence of the transition zone. Also the geoelectric section and the lithologic section were drawn and compared using the drawing menu of Microsoft Word software. This was done to facilitate wholesale graphic assessment of the parameters of each data location.

The results from the analysis of these data were supportive of the findings of the earlier work of Ademilua and Olorunfemi 2010). From these, it was discovered that the resistivity ratios allowing for detectability of the transition zone range from 1.67 to 4.33 for the HA-type curve, and 1.67 to 5.00 for the KHA-type curve, while for optimum detectability, the ratio should be between 3.0 and 3.67 for HA-type and 3.8 – 4.50 for the HA-type curve. Beyond these ranges of resistivity ratios, the transition zone becomes undetectable. The drag length was observed to increase with the thickness ratio. Furthermore, it was discovered that while the thickness ratio is independent of the resistivity ratio within the specified limits, the reverse is the case for the resistivity ratio limits, as its validity depends on keeping the corresponding thickness ratio at values not below the minimum (i.e., 0.73 for HA- and 1.10 for KHA-type curves.

Therefore, it is reasonable to infer that an increase in the thickness ratio leads to an increase in drag length. Another inference from this is that, above the minimum detectable thickness ratio, the zone would continue to be recognized on the VES curve for the same range of resistivity ratio. From the earlier results from Ademilua and Olorunfemi (2010), it was shown that the transition zone could not be detected below the thickness ratio of 0.73 for the HA- and 1.10 for the KHA-type curves. These conditions were not met as shown in Figures 3 and 4. Here, the thickness ratio is 0.59 for the HA- and 0.67 for the KHA-type curves, the zone could therefore not be detected on the respective VES curves. Furthermore, it would be discovered that the transition zone was detected on the HA- type curves where the thickness ratio is above 0.59 as shown in Figures 5 to 17.

In the second analyses, the resistivity ratio limits as obtained from the previous work are between 1.67 to 4.33 for the HA- and 1.67 to 5.00 for the KHA type curves respectively From the Figures and Table 2, it would be discovered that the resistivity ratios for all the locations complied substantially with these limits. The drag length steadily increases with increase in resistivity ratio up to an optimum value between 3.0 and 3.67 for HA-type curve and 3.80 and 4.50 for the KHA-type curve, and subsequently decrease with increase in the resistivity ratios (see Figures 18 and 19). At these optimum values, the drag length reaches its maximum and the zone becomes mostly pronounced and easily detectable on the VES curves. An increase beyond the upper limit in resistivity ratio would lead to a decrease in drag length and finally leads to undetectability of the zone on the VES curve because, the resistivity reflection coefficient (k) between the transition zone and the underlying fresh bedrock approaches +1, which makes differentiation of the zone from the fresh bedrock difficult .

Conclusively, it could be stated that, for the zone to be detectable within the resistivity ratio ranges stated above, the corresponding thickness ratios (TR1 or H'/H) must not fall below the limits specified earlier (i.e., 0.73 for the HA- and 1.10 for the KHA- type curves). In cases where the

thickness and resistivity ratio requirements are not met, the transition zone signatures were not detectable on the VES curve. These are in good agreement with the results from Ademilua and Olorunfemi (2010).

RECOMMENDATION

From the results and conclusions of the previous and current approaches to this research effort, it becomes necessary to recommend that notwithstanding the fact that the curve types and the generated models used for the previous work and the field test borehole logs and related data used for the current effort could be said to be of relatively large numbers, yet it is still considered non-exhaustive, being limited to the HA- and the KHA- type models. Also it is noted that the borehole field data are obtained from locations that are relatively few and not entirely representative of the basement complex terrain. Therefore it is recommended that future work be extended to other multi-layered earth models with type curves ending with HA- while more borehole field test data from more locations and areas than those used for this study should be obtained and used for further research and confirmatory undertakings.

APPENDICES

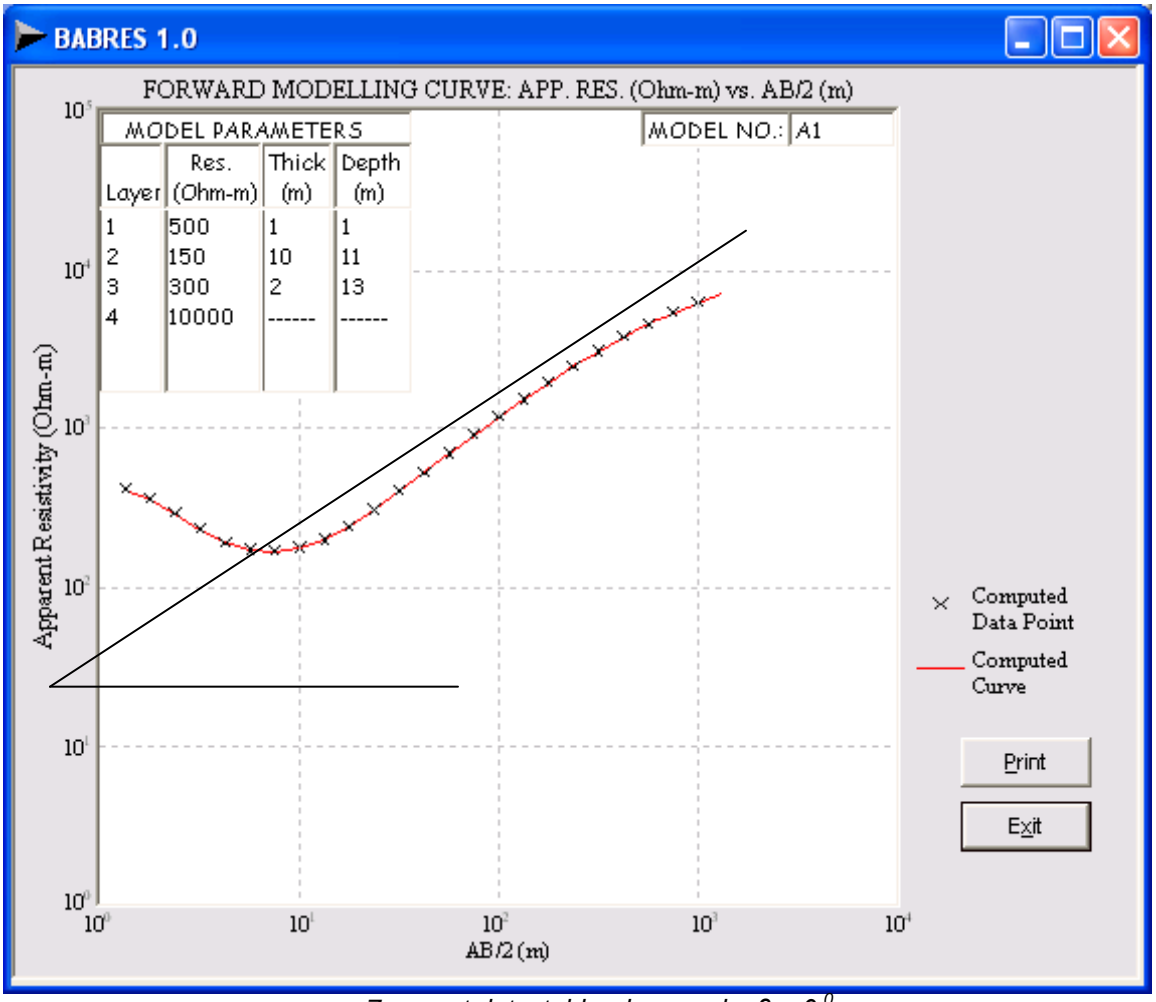

Zone not detectable, drag angle β = 0 ^{0}

Appendix 1: *Computer Model for HA-type Curve for Thickness of Transition Zone Equals 2m (Culled from Ademilua, 2007; Ademilua and Olorunfemi, 2010).*

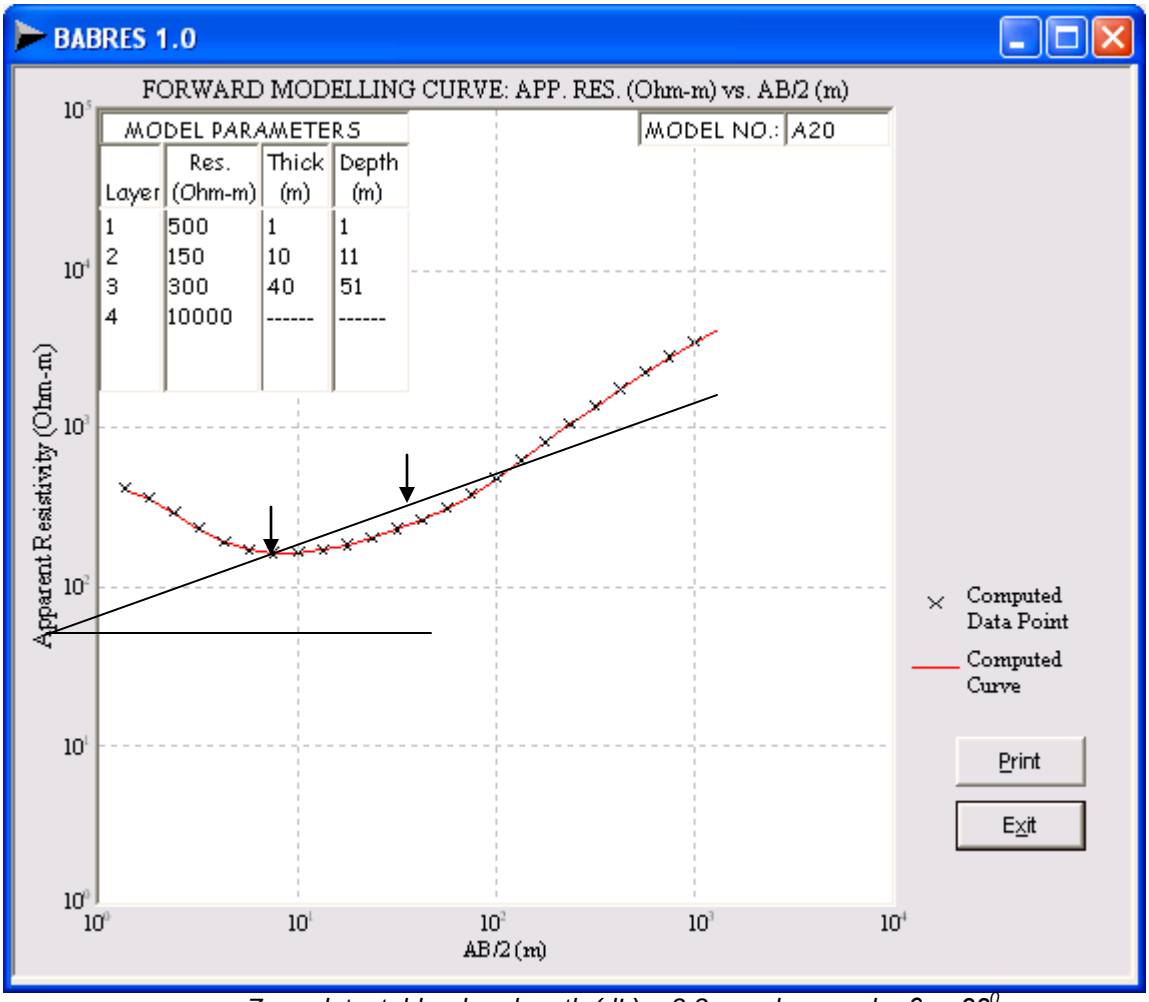

Zone detectable, drag length (dL) = 2.3cm , drag angle $\beta = 22^0$

Appendix 2: *Computer Model for HA-type Curve for Thickness of Transition Zone Equals 40m (Culled from Ademilua, 2007; Ademilua and Olorunfemi, 2010).*

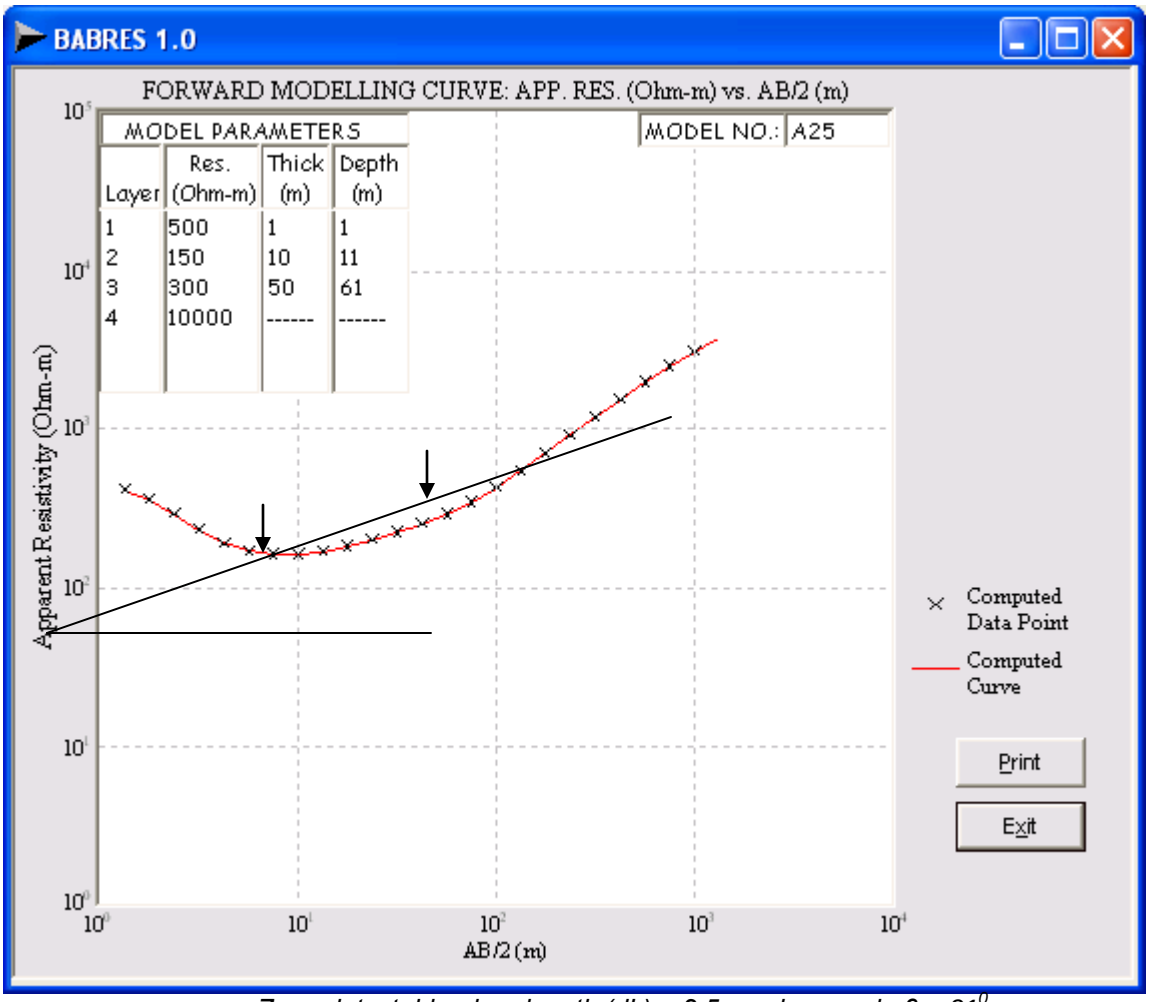

Zone detectable, drag length (dL) = 2.5cm, drag angle β = 21^0

Appendix 3: *Computer Model for HA-type Curve for Thickness of Transition Zone Equals 50m (Culled from Ademilua, 2007; Ademilua and Olorunfemi, 2010).*

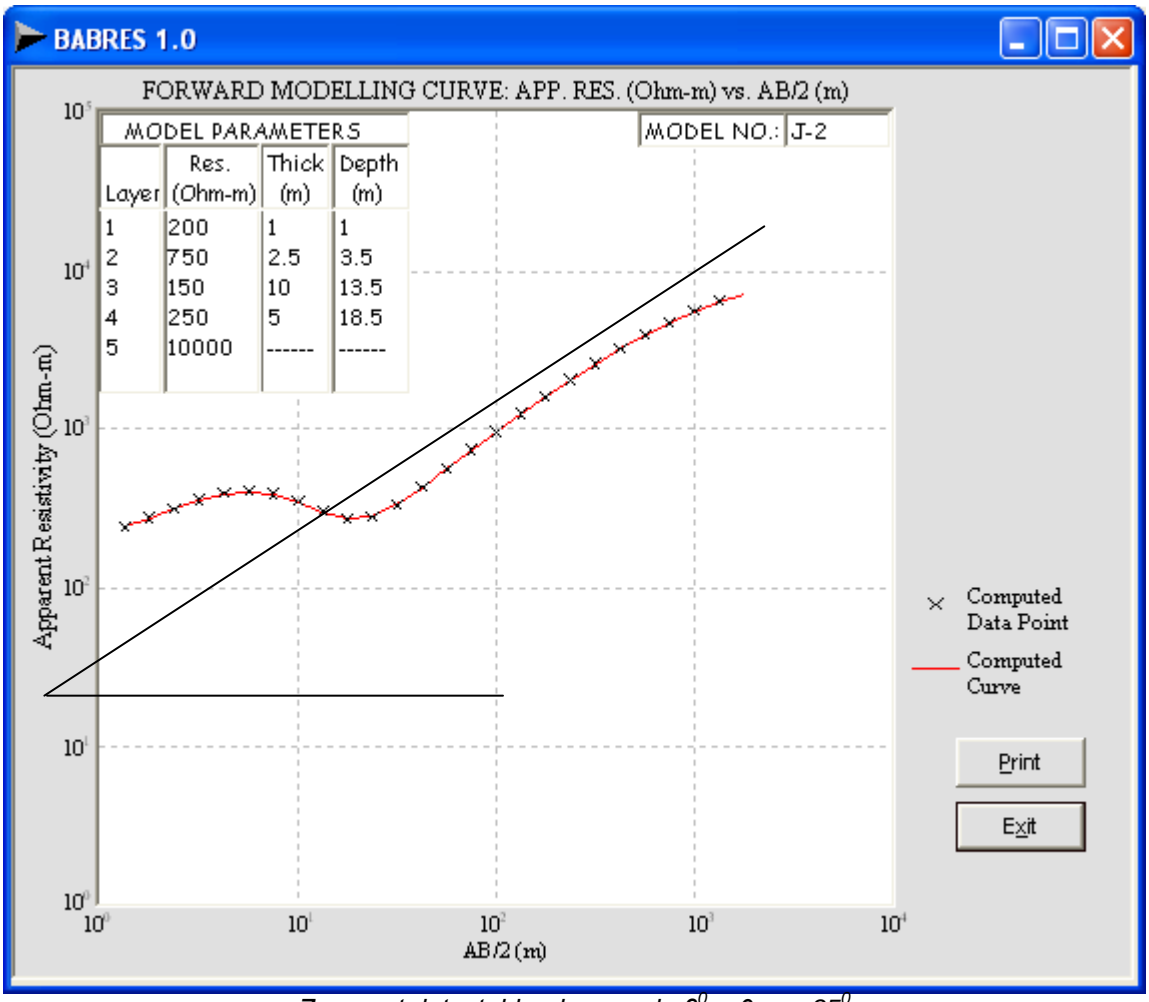

Zone not detectable, drag angle $\beta^0 = 0$, $\gamma = 35^0$

Appendix 4: *Computer Model for KHA-type Curve for Thickness of Transition Zone Equals 5m. (Culled from Ademilua, 2007; Ademilua and Olorunfemi, 2010).*

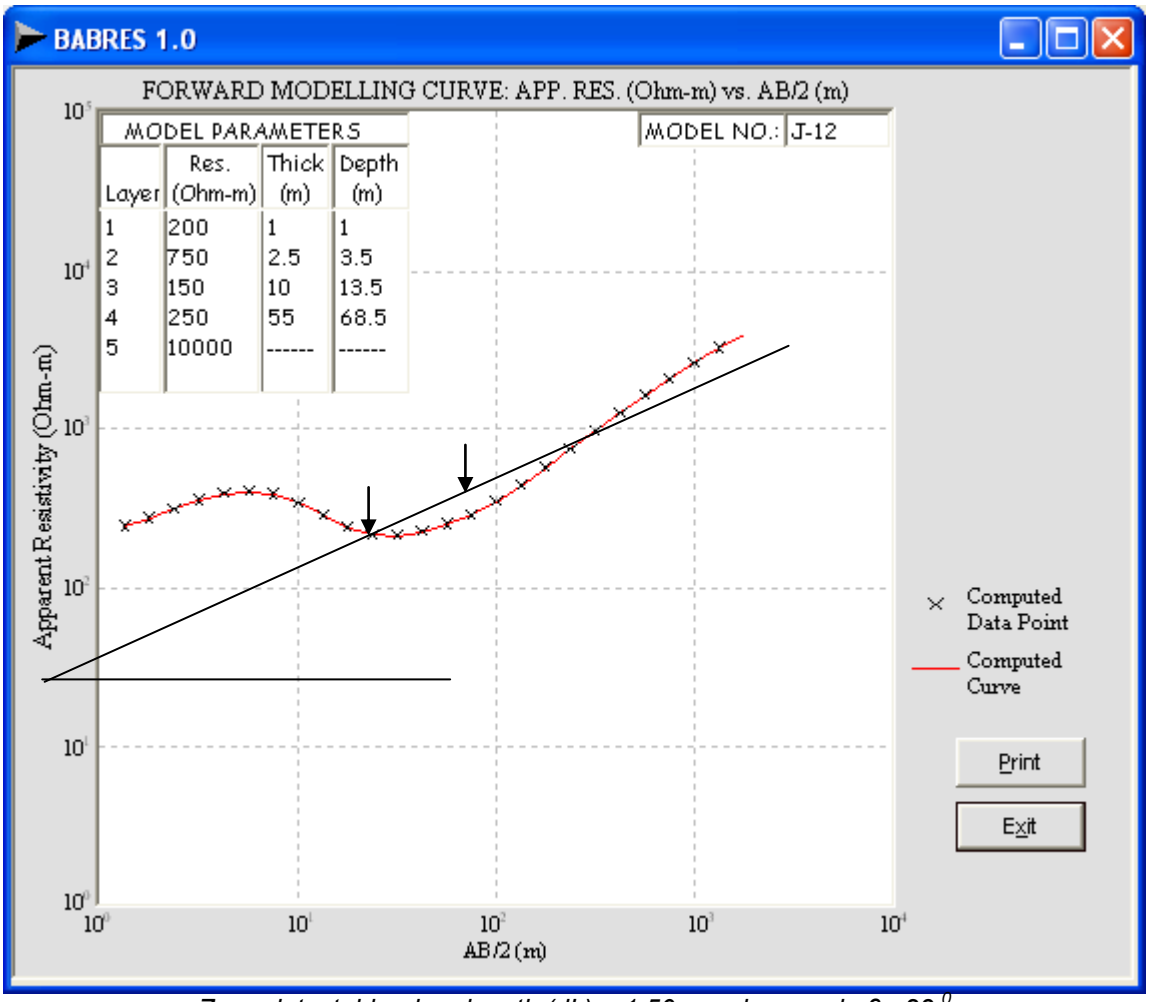

Zone detectable, drag length (dL) = 1.50 cm, drag angle β =23 ^{0}

Appendix 5: *Computer Model for KHA-type Curve for Thickness of Transition Zone Equals 55m. (Culled from Ademilua, 2007; Ademilua and Olorunfemi, 2010).*

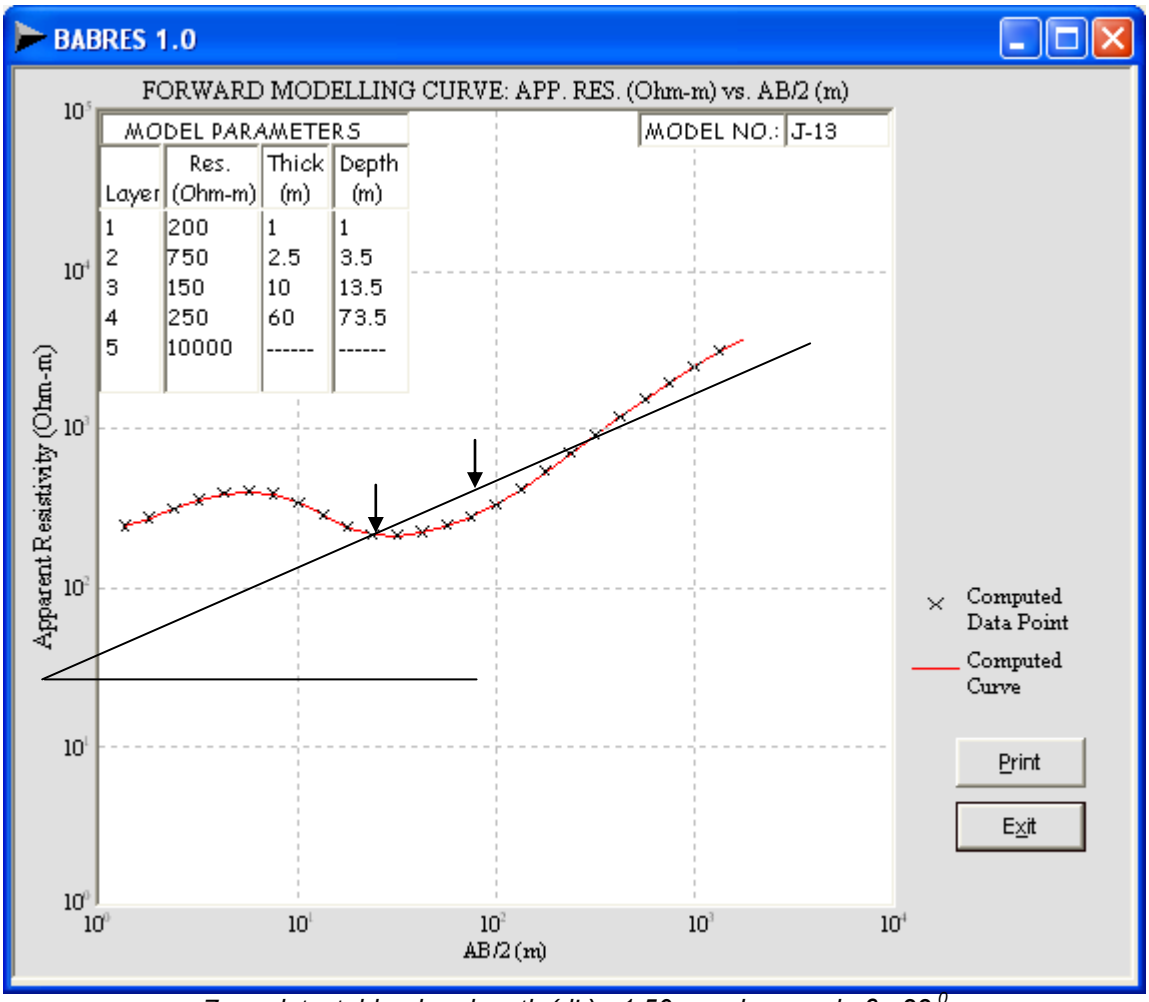

Zone detectable, drag length (dL) =1.50 cm, drag angle β =23 ^{0}

Appendix 6: *Computer Model for KHA-type Curve for Thickness of Transition Zone Equals 60m. (Culled from Ademilua, 2007; Ademilua and Olorunfemi, 2010).*

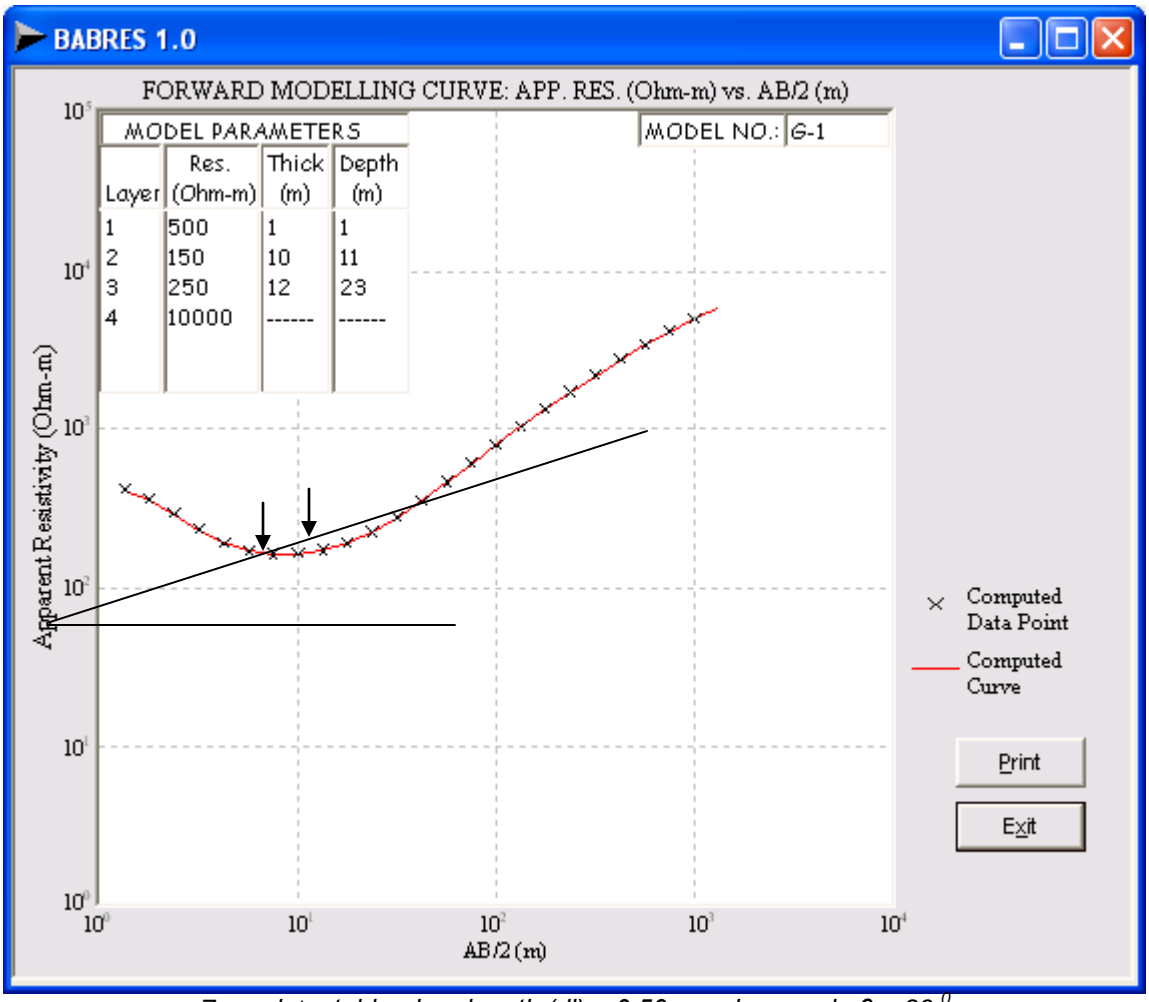

Zone detectable, drag length (dl) = 0.50 cm, drag angle β = 20 ^{0}

Appendix 7: *Computer Model for HA-type Curve for Resistivity of Transition Zone Equals 250ohm-m. (Culled from Ademilua, 2007; Ademilua and Olorunfemi, 2010).*

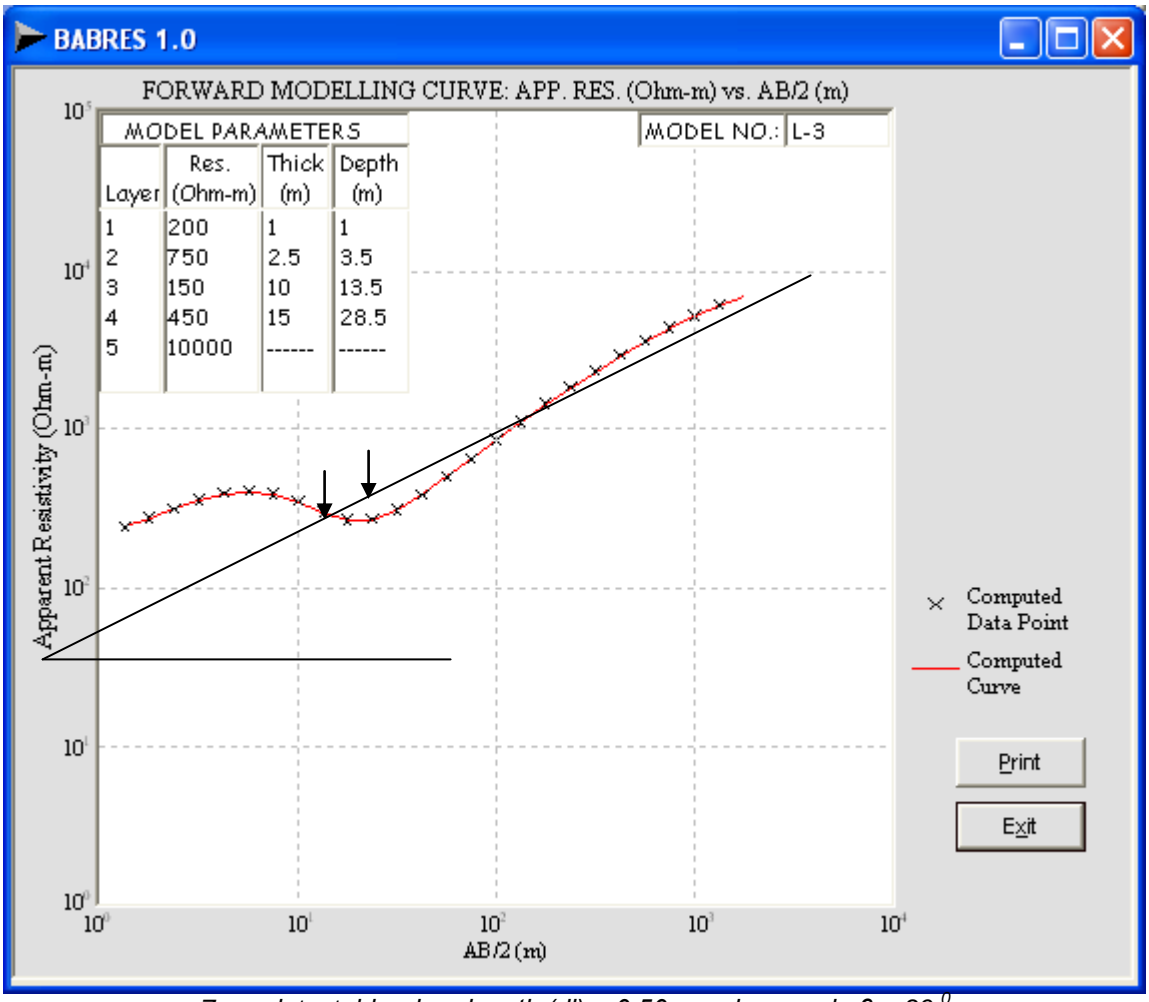

Zone detectable, drag length (dl) = 0.50 cm, drag angle β = 20 ^{0}

Appendix 8: *Computer Model for KHA-type Curve for Resistivity of Transition Zone Equals 450 ohm-m. (Culled from Ademilua, 2007; Ademilua and Olorunfemi, 2010).*

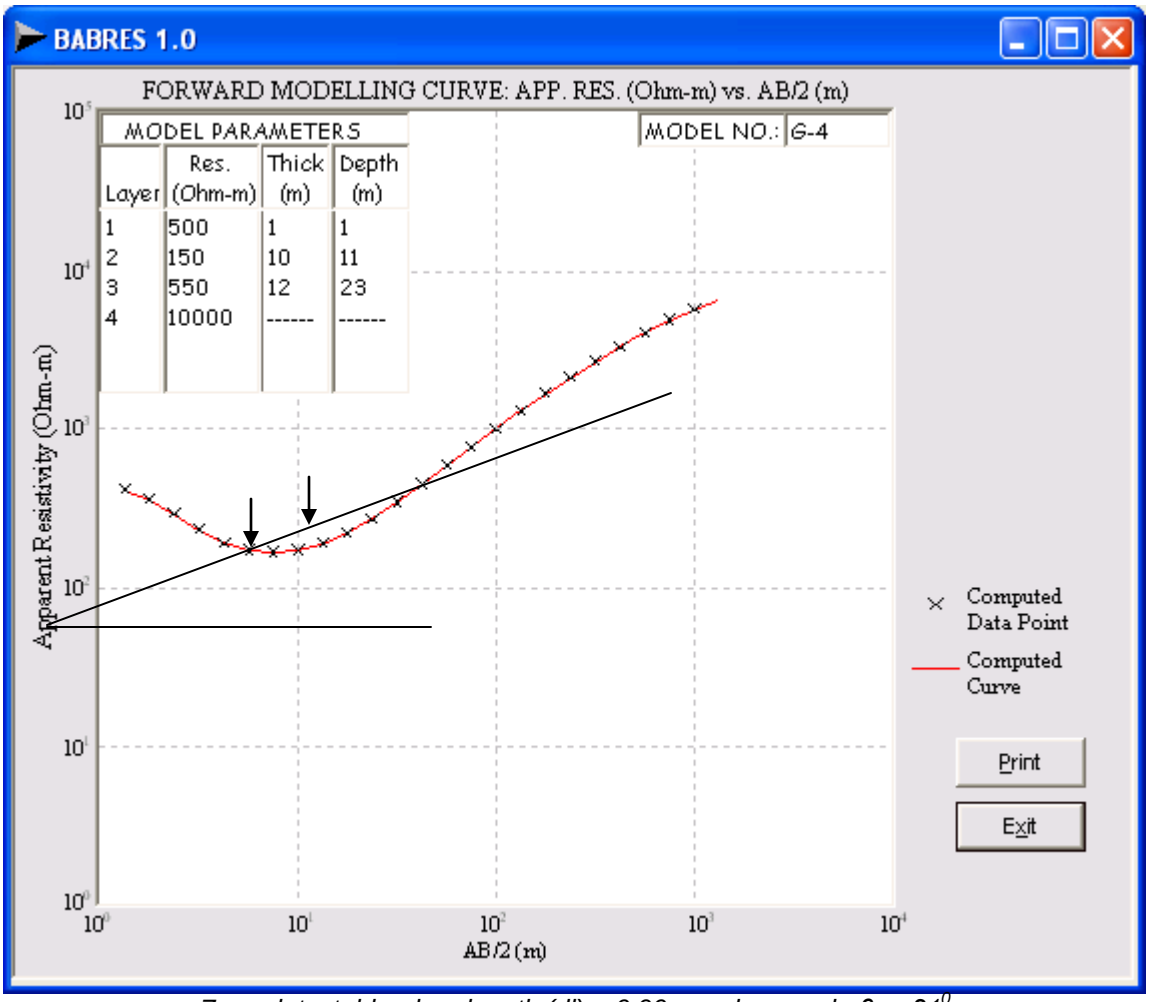

Zone detectable, drag length (dl) = 0.90 cm, drag angle β = 21^0

Appendix 9a: *Computer Model for HA-type Curve for Resistivity of Transition Zone Equals 550 ohm-m. (Culled from Ademilua, 2007; Ademilua and Olorunfemi, 2010).*

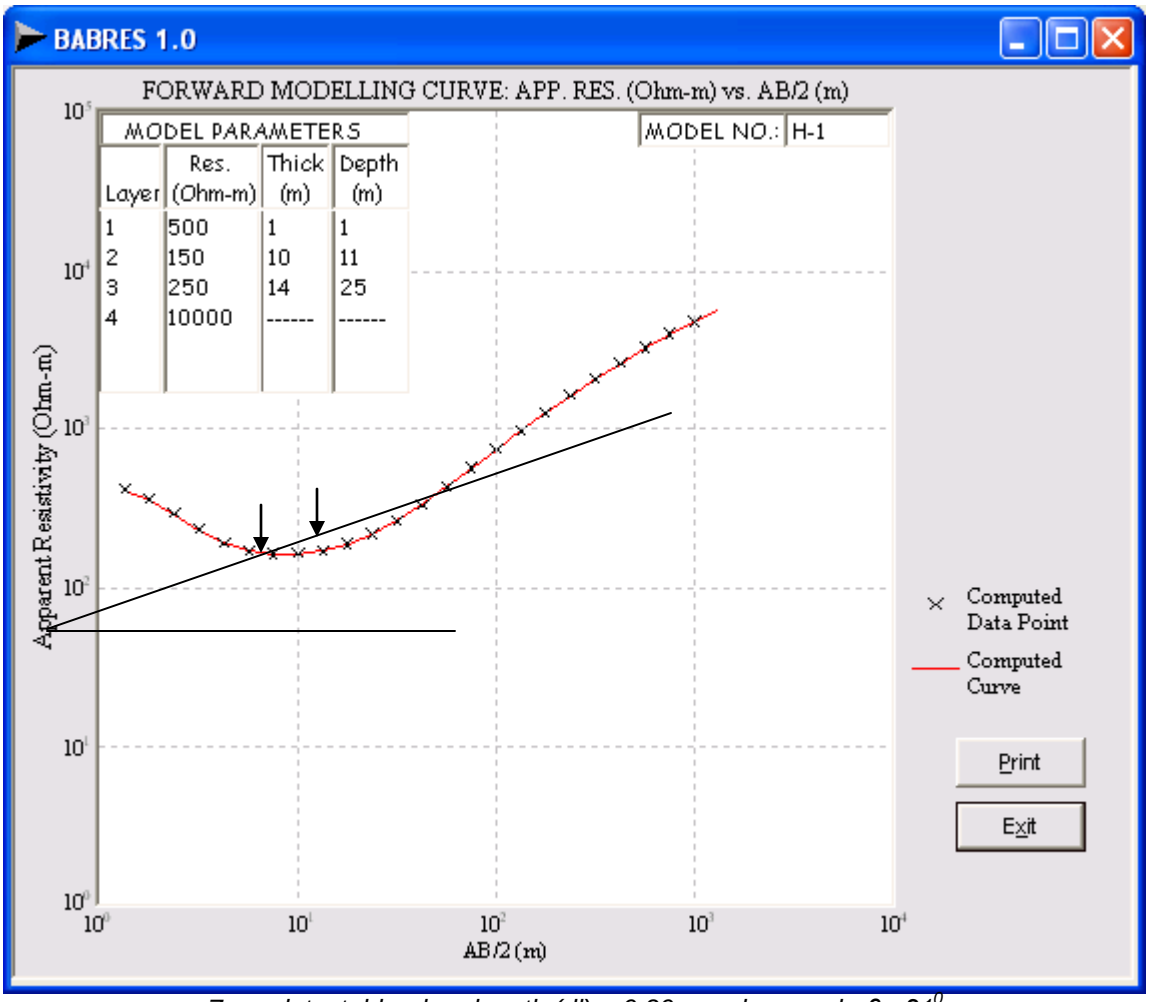

Zone detectable, drag length (dl) = 0.20 cm, drag angle β =21^0

Appendix 9b: *Computer Model for HA-type Curve for Resistivity of Transition Zone Equals 250 ohm-m. (Culled from Ademilua, 2007; Ademilua and Olorunfemi, 2010).*

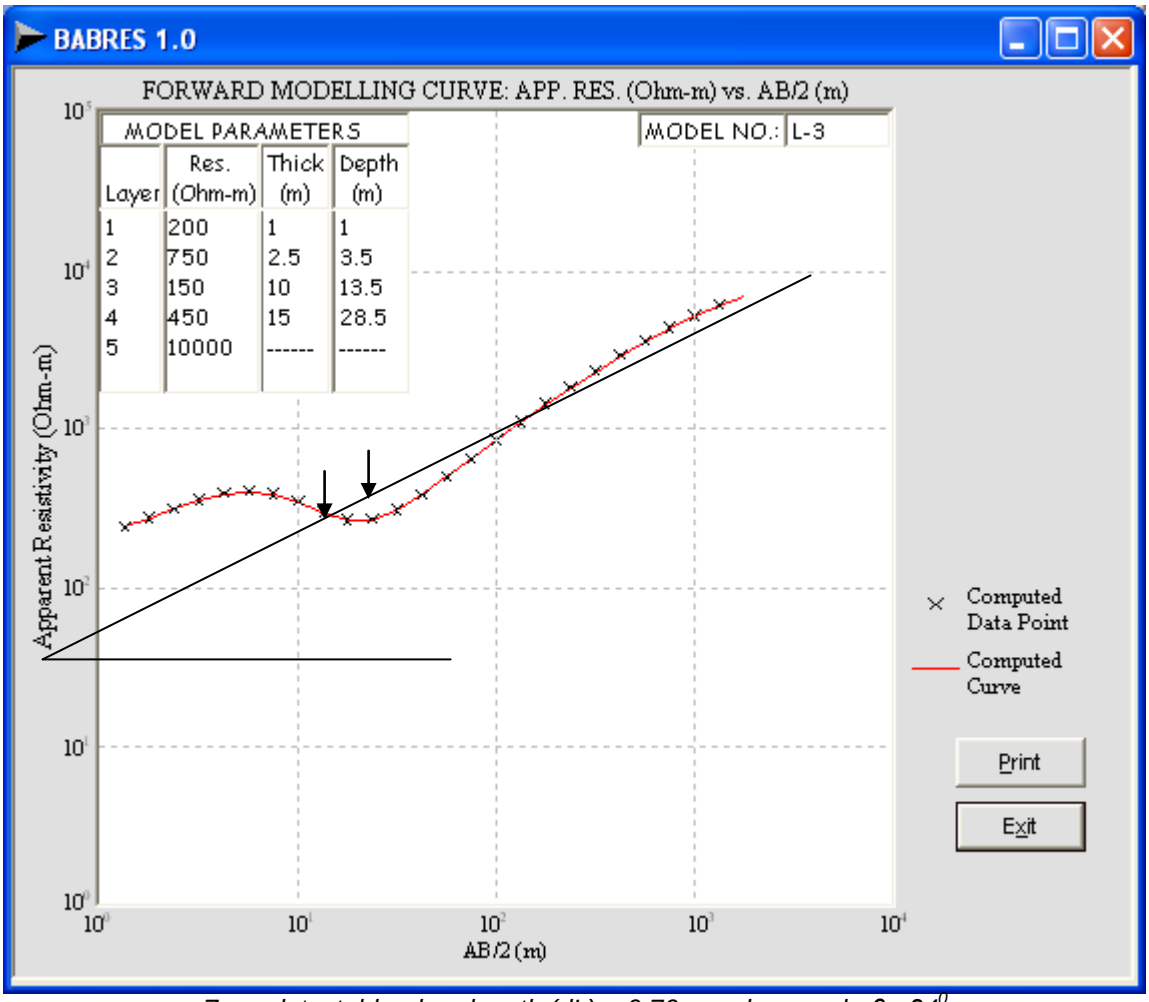

Zone detectable, drag length (dL) = 0.70 cm, drag angle β =24^0

Appendix 10: *Computer Model for KHA-type Curve for Resistivity of Transition Zone Equals 450 ohm-m. (Culled from Ademilua, 2007; Ademilua and Olorunfemi, 2010).*

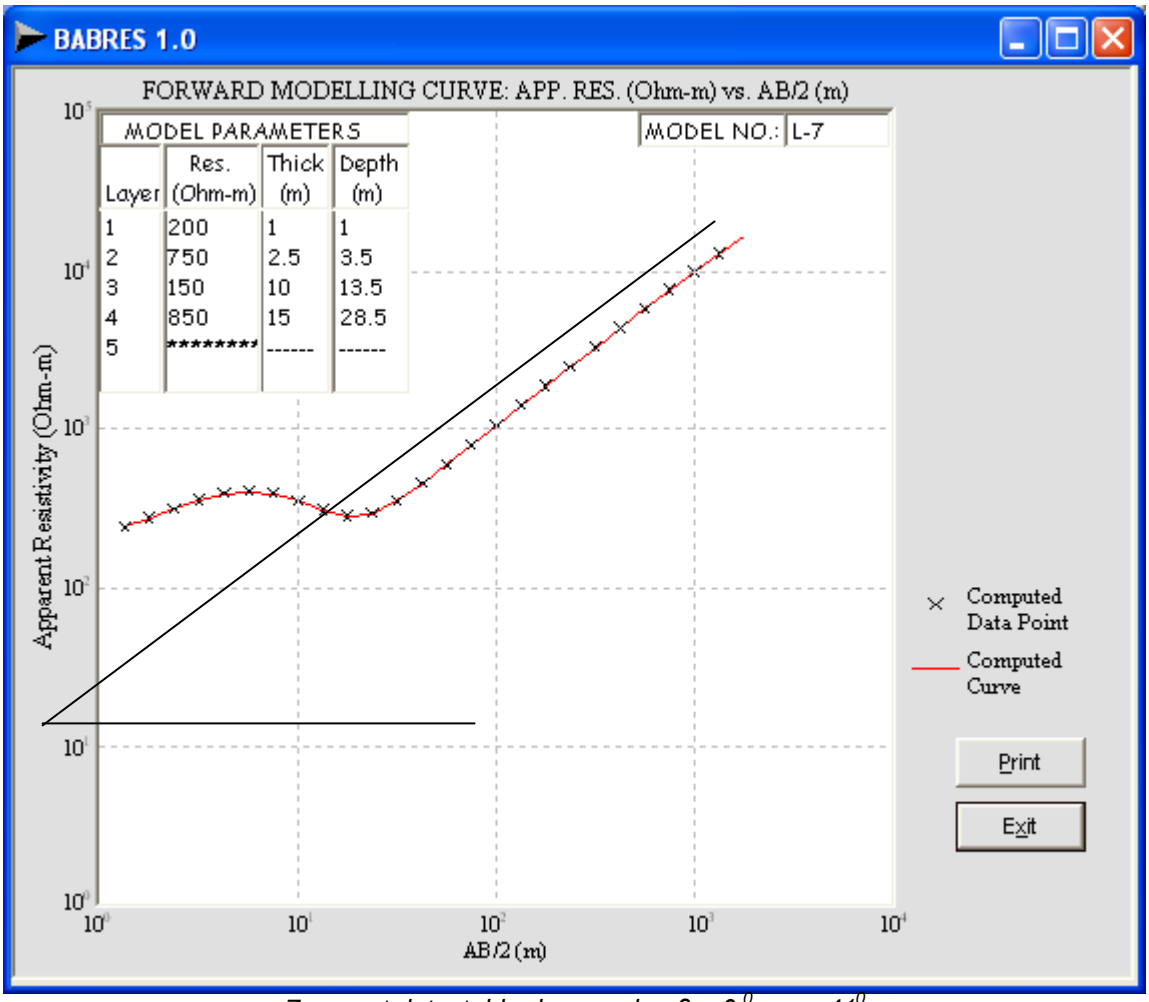

Zone not detectable drag angle $\beta = 0^0$, $\gamma = 41^0$

Appendix 11: *Computer Model for KHA-type Curve for Resistivity of Transition Zone Equals 850 ohm-m. (Culled from Ademilua, 2007; Ademilua and Olorunfemi, 2010).*

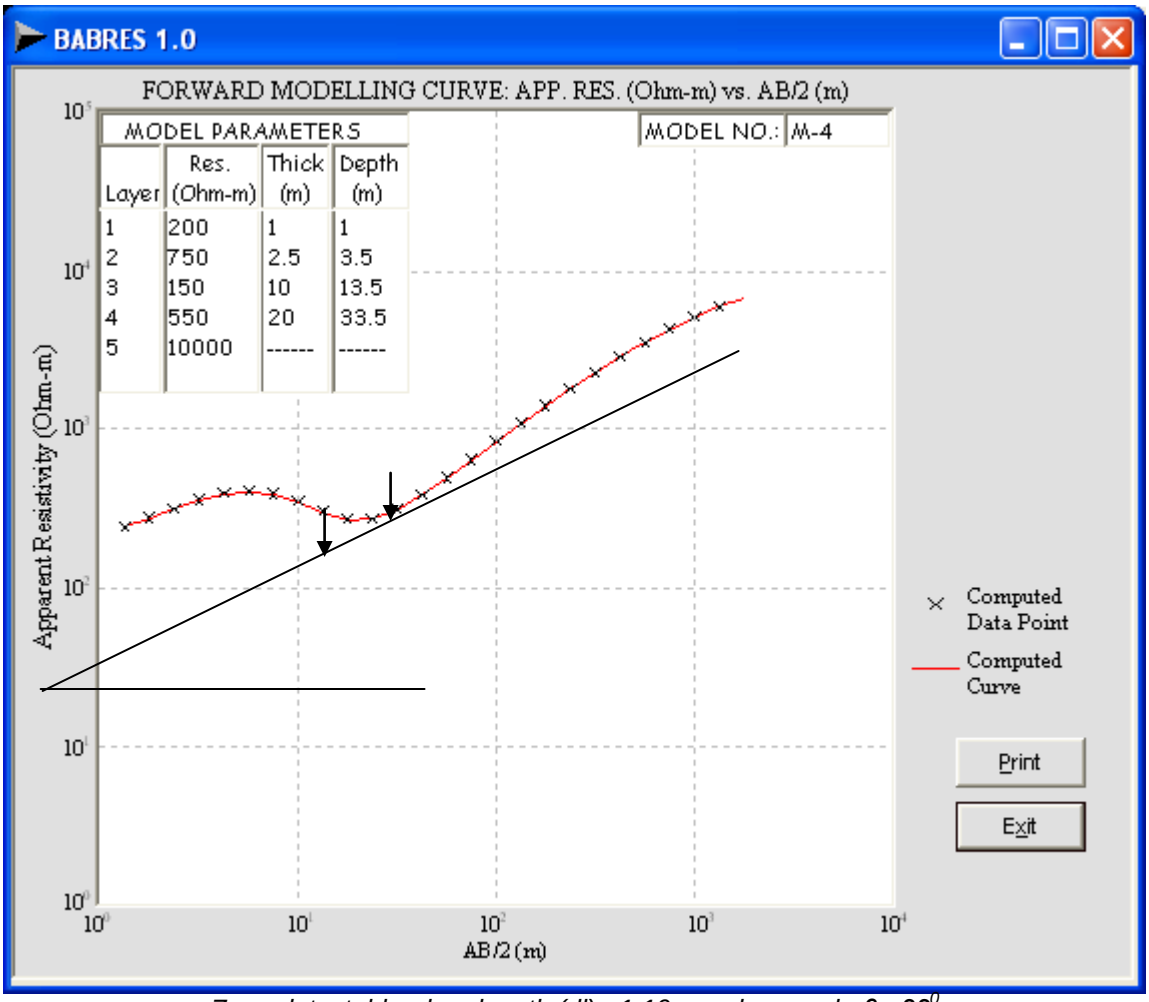

Zone detectable, drag length (dl) =1.10 cm, drag angle β =22^0

Appendix 12: *Computer Model for KHA-type Curve for Resistivity of Transition Zone Equals 550 ohm-m. (Culled from Ademilua, 2007; Ademilua and Olorunfemi, 2010).*

REFERENCES

1. Acworth, R.I. 1987. "The Development of Crystalline Basement Aquifers in Tropical Environment". *Quarterly Journal of Engineering Geology*. 20:265-272.

2. Ademilua, L.O. and M.O. Olorunfemi. 2010. "Computer Modeling for Assessing the Detectability of the Transition Zone in the Basement Complex Terrain of Southwest Nigeria". *Pacific Journal of Science and Technology*. 11(2):674-698.

3. Ademilua, O.L. 1997. "A Geoelectric/Geologic Evaluation of the Groundwater Potential of the Basement Complex Area of Ekiti and Ondo States S.W. Nigeria". Unpublished M.Sc. Thesis. Dept. of Geology, Obafemi Awolowo University: Ile-Ife, Nigeria. 130.

4. Ademilua, O.L. 2007. "Computer Modeling and Detectability Assessment of the Transition Zone in the Basement Complex Terrain of Southwest Nigeria". Unpublished Ph.D. Thesis, Dept. of Geology, Obafemi Awolowo University: Ile-Ife, Nigeria. 438.

5. Ademilua, O.L. and Olorunfemi, M.O. 2000. "A Geoelectric/Geologic and Estimation of the Groundwater Potential of Ekiti and Ondo States, Nigeria". *Journal of Technoscience*. 4:4-18.

6. Ademilua, O.L. and Olorunfemi, M.O. 2007. “An Interactive Software for SchlumbergerTheoretical Resistivity Forward Modelling”. *Journal of Applied and Environmental Sciences*. 3(2):96-107.

7. Ajayi, O., Olorunfemi, M.O., Ojo, J.S., Adegoke-Anthony, C.W., Chikwendu, K.K., Oladapo, M.I., Idornigie, A.I., and Akinluyi, F. (In Press). “Integrated Geophysical and Geotechnical Investigation of a Damsite on a River Ini, Adamawa State , Northern Nigeria. (In Press).

8. Barker, R.D., White, C.C., and Houston, J.F.T. 1990. “Borehole Siting in an African Accelerate Drought Relief Project”. In: Wright, E. P. and Burgess, W. G. (editors). *The Hydrogeology of Crystalline Basement Aquifers in Africa*. Geological Society Special Publication. No. 66: 183-201.

9. Buckley, D.K. and Zeil, P. 1987. “The Character of Fractured Rock Aquifer in Eastern Botswana”. IAHS publication No 144, 25-36.

10. Caruthers, R.M. and Smith, I.F. 1992. “The Use of Ground Electrical Survey Methods for Siting Water Supply Boreholes in Shallow Crystalline Basement Terrains”. In: Wright, E.P. and Burges, W.G. (editors). *The Hydrogeology of Crystalline Basement Aquifers in Africa*. Geological Society Special Publication. No. 66:2203-2208.

11. Hazel, J.R.T., Cratchley, C.H., and Preston, A.M. 1988. “The Location of Aquifers in Crystalline Rocks and Alluvium in Northern Nigeria with Resistivity Techniques”. *Quarterly Journal of Engineering Geology*. 21:159-175.

12. Idornigie, A.I. 2005. “Integration of Geophysical and Remotely Sensed Data Sets in Site Characterization”. Unpublished Ph.D. Thesis. Geology Dept. O.A.U.: Ile-Ife, Nigeria. 246.

13. MacFarlane, M.J. 1989. “Groundwater Exploration and Development in Crystalline Basement Aquifers”. *Proceedings of Commonwealth Science Council*. Zimbabwe.

14. Ojo, J.S., Ayangbesan, T.A., and Olorunfemi, M.O. 1990. “Geophysical Survey of a Damsite: A Case Study”. *Journal of Min. and Geol*. 26(2): 201-296.

15. Olayinka, A.I. and Oladipo, A.O. 1994. “A Quantitative Assessment of Geoelectrical Suppression in Four- Layer HA-type Earth Model”. *Journal of Min. and Geology*. 30(2):251-258.

16. Olorunfemi, M.O. and Fasuyi, A.S. 1993. “Aquifer Types and the Geoelectric/Hydrogeologic Characteristics of the Basement Terrain of Niger State, Nigeria”. *Journal of African Earth Sciences*. 16(3):309-317.

17. Olorunfemi, M.O., Idornigie, A.I., Fagunloye, H.O., and Ogun, O.A. (In Press). “Assessment of Anomalous Seepage Conditions in the Opa Dam Embankment, Ile-Ife Southwestern Nigeria.

18. Western, C.J. 1997. “Tools for Map Analysis Applied to the Selection of Waste Disposal Site”. *ILWIS Applications Guide*. ITC, Enschede: The Netherlands. 219-237.

19. White, C.C., Houston, J.F.T., and Barker, R.D. 1988. “The Victoria Province Drought Relief Project Geophysical Siting of Borehole. *Groundwater*. 26:309-316.

20. Zohdy, A.A.R., Easton, G.P., and Mabey, D.R. 1974. “Application of Surface Geophysics to Groundwater Investigations”. *U.S. Geological Survey Techniques of Water Resources Investigations*. Book 2, Chapter D1. USGS: Washington, D.C.

ABOUT THE AUTHORS

Ademilua Oladimeji Lawrence received his M.Sc. and Ph.D. in Applied Geophysics from the Obafemi Awolowo University, Ile–Ife Nigeria, and he has published several research papers in both local and international journals. He is currently a Lecturer Grade 1 at the Geology Department of the University of Ado Ekiti Nigeria.

Olorunfemi Martins Olu received his B.Sc., from the University of Ife, Ile-Ife, Nigeria, after which he proceeded to the University of Birmingham, U.K., for his M.Sc. and Ph.D., both in Applied Geophysics. He has edited several journals at the local, national, and international levels. He is currently a Professor of Applied Geophysics at the Geology Department of the Obafemi Awolowo University Ile-Ife, Nigeria.

SUGGESTED CITATION

Ademilua, L.O. and M.O. Olorunfemi. 2011. “Further Reflections on Computer Modeling for Detectability Assessment of the Transition Zone in the Basement Complex Terrain of Southwest Nigeria”. *Pacific Journal of Science and Technology*. 12(1):435-471.

Pacific Journal of Science and Technology